NOAA Technical Report ERL 414-AOML 30

Tropical Cyclone Modification: The Project Stormfury Hypothesis

Robert C. Sheets

August 1981

QC
807.5
U66
no. 414
AOML 30

U.S. Department of Commerce
National Oceanic and Atmospheric Administration
Environmental Research Laboratories

QC
807.5
.U66
no.
414
c.2

NOAA Technical Report ERL 414-AOML 30

Tropical Cyclone Modification: The Project Stormfury Hypothesis

Robert C. Sheets

Atlantic Oceanographic and Meteorological Laboratories
Miami, Florida

August 1981

U.S. Department of Commerce
Malcolm Baldrige, Secretary

National Oceanic and Atmospheric Administration
John V. Byrne, Administrator

Environmental Research Laboratories
Boulder, Colorado
George H. Ludwig, Director

University of
Miami Library
4600 Rickenbacker Causeway
Miami, Florida 33149

014199

NOTICE

Mention of a commercial company or product does not constitute an endorsement by NOAA Environmental Research Laboratories. Use for publicity or advertising purposes of information from this publication concerning proprietary products or the tests of such products is not authorized.

CONTENTS

Page

ABSTRACT 1

1. THE PHYSICAL BASIS OF THE STORMFURY HYPOTHESIS 1

2. EXPERIMENTAL SEEDING RESULTS 6

3. POSSIBLE EFFECTS OF STORMFURY EXPERIMENTS 8

3.1 Track 9

3.2 Rainfall 17

3.3 Wind Field 19

3.4 Storm Surge 24

4. EXPERIMENT DESIGN 27

5. POTENTIAL BENEFITS 32

6. SUMMARY 34

7. ACKNOWLEDGMENTS 34

8. REFERENCES 34

Appendix A: Effects of Seeding on Tropical Cyclone Motion 38

Appendix B: Tropical Cyclone Rain Estimation From Geosynchronous Satellite Imagery 45

Appendix C: Simulations of Tropical Cyclone Rainfall Distribution Changes Based on the Stormfury Hypothesis 47

TROPICAL CYCLONE MODIFICATION: THE PROJECT STORMFURY HYPOTHESIS

Robert C. Sheets

ABSTRACT. The Project Stormfury modification theory, its physical basis, and the experiment design are described, and the possible effects of such experiments on tropical cyclone motion, rainfall, wind fields, and storm surge are examined. Studies of natural storm variability, exploratory experiments, sensitivity tests, numerical simulations, and theoretical calculations indicate that experiments conducted according to the Stormfury hypothesis could result in reductions of 10% to 15% in the maximum windspeed and associated damage reductions of 20% to 60%, with no apparent significant and/or detectable effect on storm motion or net rainfall accumulated areawide or at specific locations for a moving storm.

1. THE PHYSICAL BASIS OF THE STORMFURY HYPOTHESIS

Methods proposed for modifying tropical cyclones include those without any reasonable physical basis, those that may be scientifically sound, but are apparently logistically impractical, and those that appear to be both scientifically sound and feasible. The methods that appear to be scientifically sound can be divided into two classes: those that attempt to reduce the latent and sensible heat transfer from the ocean to the atmosphere and those that attempt to alter the convective cloud distributions and, therefore, the flow through the storm. The storm modification method discussed here is the latter type and is known as the Stormfury hypothesis.

Project Stormfury experiments are designed to cause a reduction in the maximum windspeeds by altering the location of the transverse circulation near the storm's center. At low levels, the warm, moist air spirals over the tropical sea toward the storm's center, acquiring copious quantities of latent and sensible heat from the sea. The inflowing air, already turning slowly in the direction of the Earth's rotation at large radii before it starts its inward spiral, gathers tangential speed through partial conservation of its absolute angular momentum as it draws nearer the storm's center, and often produces winds with speeds greater than 50 m s^{-1}. Large portions of this air flow upward into the eyewall (a band of clouds ringing the relatively calm eye) and into surrounding rainbands. The rising air cools, and latent heat is released through the condensation process as clouds and precipitation form, thus furnishing most of the energy for driving the storm before the air moves away from the storm's core at high levels.

The small areal extent of this convective-scale ascent of air from the inflow layer to the upper tropospheric outflow layer, when compared with the total area of the hurricane, generally is not appreciated and is worth illustrating (Sheets and LaSeur, 1979). Simple geometric considerations (fig. 1), combined with mass continuity, lead to the results given in table 1, which show that only a fraction of an annular eyewall can contain convective-scale

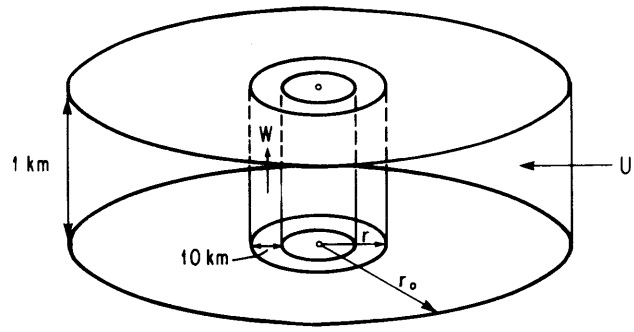

Figure 1.--Convective-scale ascent of air from the inflow layer to the upper tropospheric outflow layer of a tropical storm.

updrafts in the range of 10 to 20 m s^{-1}, speeds that have been measured in tropical cyclones. For example, if the inflow in the boundary layer averaged around the storm through a depth of 1 km is 1 m s^{-1} at a radius r_o, equal to four times the radius of maximum winds r, then only 4% of a 10-km-wide annular ring centered at r would have to contain 10 m s^{-1} updrafts to evacuate the total mass inflow. Furthermore, when one considers the ratio of the eyewall convective area (active updrafts) to the total area within three or four times the radius of maximum winds (region containing most of the concentrated convection), the typical value is less than 1%. This factor has important consequences for proposed Stormfury experiments, because it implies that only a relatively small region of the storm needs to be modified to produce a significant result (that is, the experiment appears to be logistically feasible).

Another important consideration is whether the convective-scale ascent can be modified so that significant changes occur in the location and intensity of the vertical mass transport in the tropical cyclone. The method for altering the convective-scale ascent proposed under Project Stormfury is dynamic seeding. This technique has proved effective for causing cloud growth in tropical regions (Simpson et al., 1967) but remains to be proved in the tropical cyclone environment. Observations in hurricanes give good reason to expect that the technique will work. For instance, hurricanes that have a well-formed eyewall often contain convective clouds in areas that are outward from the eyewall and that do not extend to the outflow level. Other observations indicate that many of these clouds contain large quantities of

Table 1.--Percent of annular ring 10-km wide centered at radius r containing updraft speeds necessary to transport vertically an assumed horizontal inflow of 1 m s^{-1} averaged over a depth of 1 km around the storm at a radius of r_o

Ratio (r_o/r) \ Necessary updraft speed (m s^{-1})	Percent				
	5	10	15	20	25
2	4	2	1.3	1	0.8
4	8	4	2.6	2	1.6
6	12	6	4	3	2.4
8	16	8	5.3	4	3.2
10	20	10	6.7	5	4

supercooled liquid water (Sheets, 1969a). Calculations based on buoyancy indicate that these clouds may be caused to grow through the dynamic seeding process hypothesized below (Sheets, 1969b). Injection of silver iodide particles into the upper portion of these clouds causes the droplets to freeze, releasing the latent heat of fusion. This additional heat causes this portion of the cloud to be warmer and, therefore, lighter than the surrounding air, thus triggering an increase in the ascending flow. Additional warm, moist air is diverted into the growing cloud, and as this new air rises, it expands and cools, and additional water vapor condenses or sublimates, releasing considerably more latent heat than does the initial freezing caused by the seeding. Hence, the seeded cloud is expected to grow to the outflow level, providing a new convective conduit for the vertical transport of the inflowing, low-level air. This process is schematically illustrated in figs. 2 and 3. The top panel of fig. 2 illustrates the initial structure of the storm before the start of the seeding. Note the well-formed eyewall. The middle panel hypothetically represents the stage where the seeding effect is taking place. Here the initial eyewall is weakened because the low-level, inflowing, warm, moist air that maintains these clouds is being diverted upward in the seeded cloud. The bottom panel illustrates the final, modified stage of the hypothesized sequence of events. The old eyewall has now dissipated and the seeded clouds become the new eyewall, providing a new conduit for the major vertical mass flow through the hurricane. Figure 3 is an enlarged version of the right side of fig. 2, showing the detailed cloud structure and transverse circulation during the hypothesized sequence of events. This hypothesized sequence of events is summarized as follows:

(1) Clouds are seeded outward (away from the storm center) from the external edge of a mature hurricane eyewall.

(2) The supercooled water in the seeded clouds freezes, latent heat of fusion is released, and the buoyancy of the upper portion of the cloud increases, resulting first in increased ascent in the seeded portion of the clouds and then in increased ascent throughout the cloud and increased cloud base convergence. These changes further result in increased condensation rates and cloud growth.

(3) The seeded clouds grow to the outflow level, providing a major new conduit for vertical mass transport.

(4) The old eyewall circulation weakens as the major vertical mass transport is diverted to the seeded clouds.

(5) The maximum windspeeds are reduced because of the outward shift of the radius of maximum winds (region of maximum vertical mass transport) and the principles of the partial conservation of angular momentum.

(6) The pressure field adjusts to the new wind field.

(7) The storm starts to return to its natural state, as determined by the synoptic-scale environment (atmospheric and oceanic conditions over and in which the hurricane is embedded), 6 to 18 h after the final seeding (based on Hurricane Debbie results [Gentry, 1970] and on numerical simulations). Note that this is a hypothesized dynamic effect rather than the thermal effect postulated in the Stormfury hypothesis originally proposed by Simpson et al. (1963). That is, the released latent heat in the seeded cloud is postulated to manifest itself quickly into localized increases in buoyancy. The pressure field then is postulated to adjust to changes in the wind field rather than to direct thermal effects.

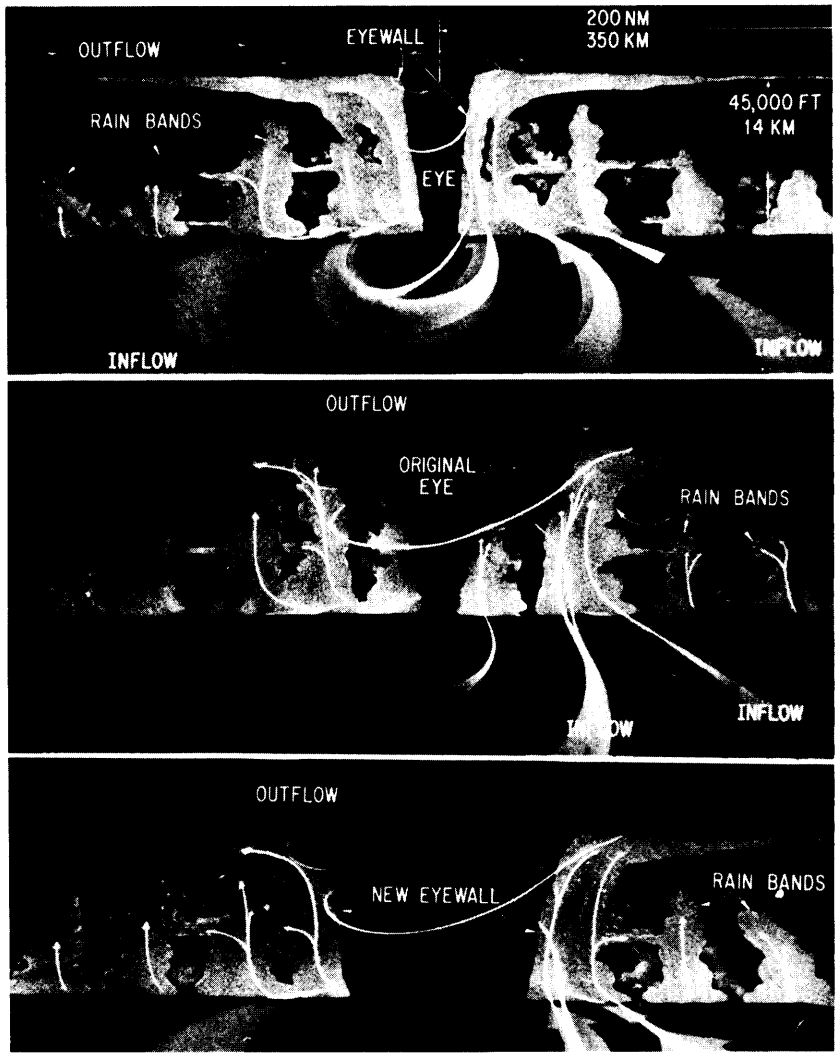

Figure 2.--Vertical cross section of a hurricane, showing the hypothesized storm structure before (top), during (middle), and after (bottom) the seeding operation.

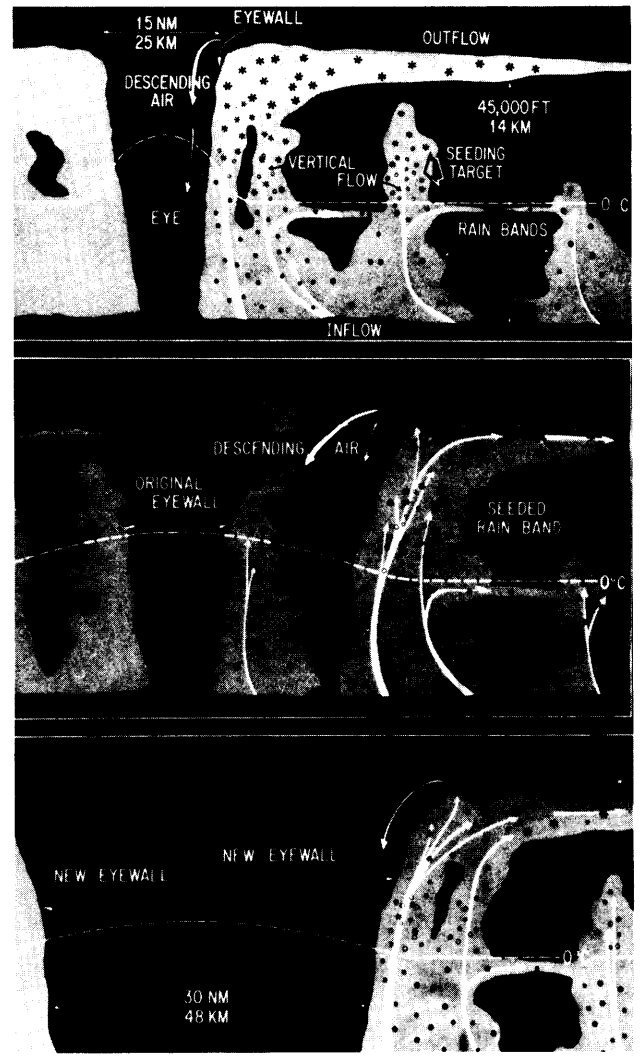

Figure 3.--Enlarged section of the right side of fig. 2, illustrating the detailed cloud structure and hypothesized seeding effect.

Table 2.--Potential reduction of windspeed (%) at a radius r that is greater than some initial radius r_o, if $V_o r^x$ = constant

Ratio (r/r_o) \ x	Percent reduction					
	0.5	0.6	0.7	0.8	0.9	1.0
1.2	9	10	12	14	15	17
1.4	15	18	21	24	26	29
1.6	21	25	28	31	35	37
1.8	25	30	34	38	41	44
2.0	29	34	38	43	46	50

Possible reductions in maximum wind are listed in table 2. The values are based on the relationship $V_\theta r^x$ = constant where V_θ is the tangential wind, r is the radial distance from the center of circulation, and x is a variable depending on storm characteristics. Both observational and theoretical evidence support the relationships used in deriving this table. If there were no losses of momentum to the ocean as the air flowed into the hurricane, the variation of wind with radius for some distance outward from the eyewall maximum would be very nearly inversely proportional to the radius (i.e., x = 1). Since there are frictional losses of momentum to the sea and surrounding air, the variation is nearly inversely proportional to r^x where x ranges from perhaps 0.4 to 0.8, depending on the rate of frictional loss of momentum. An example of a windspeed profile that illustrates these characteristics is shown in fig. 4 where x = 0.5 and 0.6 for Hurricane Anita on September 2, 1977. If the inflowing air could be induced to rise in enhanced convective updrafts at a radius 40% to 80% larger than the preexisting eyewall, the maximum winds could be reduced 15% to 30%.

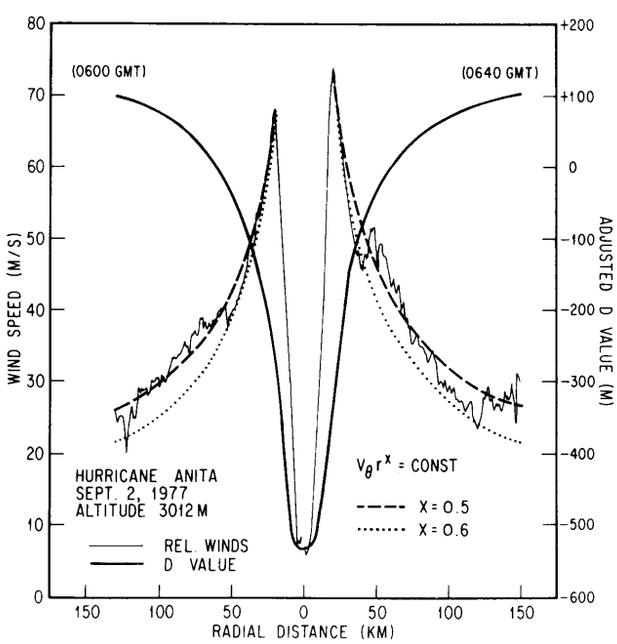

Figure 4.--Sample windspeed and adjusted D value (a measure of pressure) profiles with computed wind profiles of $V_\theta r^x$ = constant for x = 0.5 and 0.6.

2. EXPERIMENTAL SEEDING RESULTS

The tracks of all storms seeded in Stormfury experiments from 1961 through 1979 are illustrated in fig. 5. (Only the two Hurricane Debbie experiments were conducted in a manner that closely followed the present Stormfury hypothesis.) All experiments to date are summarized in table 3.

The first storm seeded was Hurricane Esther in 1961. Clouds near the eyewall were seeded on September 16 and 17, 1961, with relatively small amounts of silver iodide. An apparent 10% reduction in the maximum windspeed was recorded after seeding on the 16th, but little change was observed on the

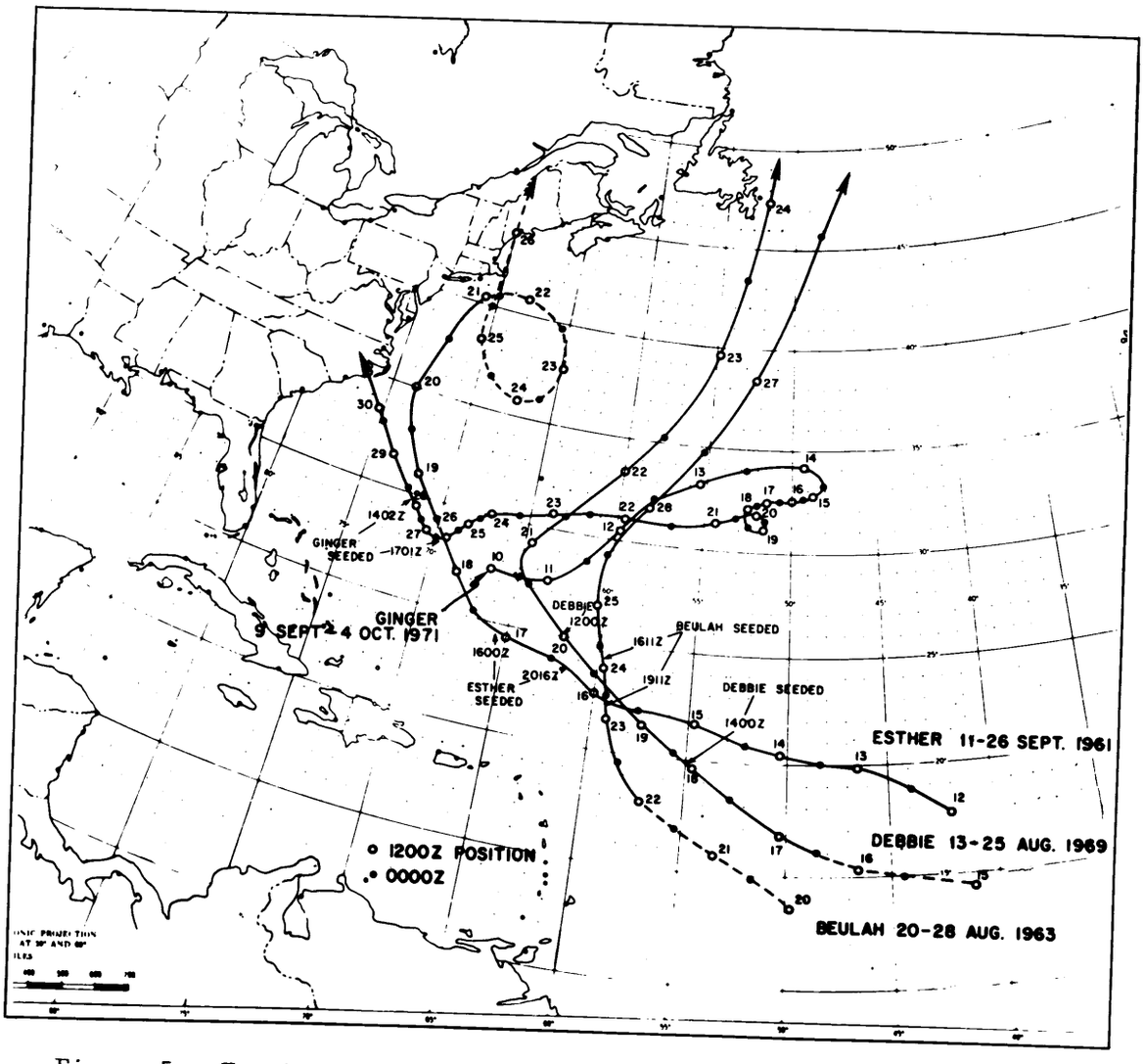

Figure 5.--Tracks of all hurricanes seeded from 1961 through 1979. Times and locations of seedings are indicated.

Table 3.--Summary of experimental results of seeding hurricane clouds near the eyewall*

Hurricane**	Date	No. of seedings	Silver iodide used† (no./kg)	Approx. max. windspeed change (%)
Esther	Sept. 16, 1961	1	8/35.13	-10
Esther	Sept. 17, 1961	1	8/35.13	0††
Beulah	Aug. 23, 1963	1	55/219.96	0††
Beulah	Aug. 24, 1963	1	67/235.03	-14
Debbie	Aug. 18, 1969	5	976/185.44	-30
Debbie	Aug. 20, 1969	5	978/185.82	-15

*Gentry (1974)

**Note: Seedings of a hurricane on October 13, 1947, and of Hurricane Ginger on September 26 and 28, 1971, are not included. The clouds seeded in these storms were far different from those in the storms listed above, and the seedings were performed differently.

†Values are total units and total kilograms of silver iodide used each day.

††Pyrotechnics dropped outside seedable clouds.

17th, when the silver iodide was apparently dropped in a cloud-free zone (Simpson et al., 1963). Similar single seeding experiments with similar results were conducted in Hurricane Beulah on August 23 and 24, 1963. A 10% to 14% apparent reduction of maximum windspeed was noted on August 24, whereas little change was observed on the 23rd (Simpson and Malkus, 1964). Postexperimental analyses indicated that the seeding agent was dropped in a relatively cloud-free zone on the 23rd, as it was in the Esther case on the 17th. These errors in delivery of the seeding agent were caused primarily by poor radar systems.

The Hurricane Debbie experiments conducted on August 18 and 20, 1969, appear to have been the most successful and are the only ones conducted to date that closely follow the present Stormfury hypothesis. Maximum windspeed reductions of 30% and 15% were well documented (figs. 6 and 7). The windspeeds were near 50 m s^{-1} (100 kn) before the seeding experiment began on August 18. The storm was then seeded five times, with 2 h between each seeding event over the next 8 h. By the end of the monitoring period, 4 to 6 h after the final seeding, the maximum recorded winds were near 35 m s^{-1} (70 kn).

Hurricane Debbie was not seeded on August 19 and regained strength. By early morning on August 20, the maximum windspeeds were again near 50 m s^{-1} (100 kn). The storm again was seeded five times, with approximately 2 h between each seeding. Maximum windspeeds were observed to decrease after the

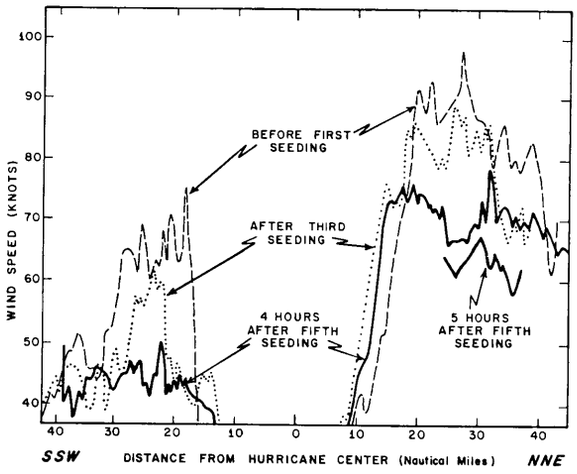

Figure 6.--Hurricane Debbie wind-speed profiles at 12,000 ft, recorded on August 18, 1969 (Gentry, 1970).

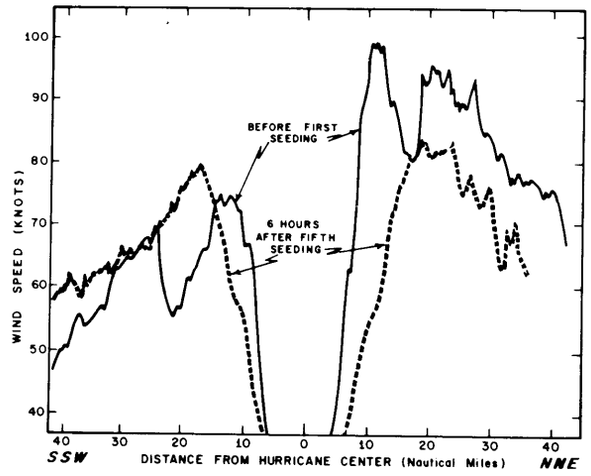

Figure 7.--Hurricane Debbie wind-speed profiles at 12,000 ft, recorded on August 20, 1969 (Gentry, 1970).

seeding operation, with peak winds of 42 m s^{-1} (85 kn) recorded at the end of the monitoring period about 4 to 6 h after the final seeding. Even though analyses by Hawkins (1971) and Sheets (1973) seem to indicate that a portion of the windspeed reduction recorded on August 18 was caused by synoptic-scale influences, these analyses also strongly suggest that significant reductions resulted, on both days, that could reasonably be attributed to the seeding events.

Hurricane Ginger (1971) seeding experiments were conducted in an outer rainband (not in the manner of the Stormfury eyewall experiments). Only some localized cloud structure changes were noted. There was no detectable effect on the wind field.

3. POSSIBLE EFFECTS OF STORMFURY EXPERIMENTS

The primary questions about experiments conducted in hurricanes concern possible effects on the storm's track, rainfall, wind field, and associated storm surge. These aspects of the experiments can be addressed through (a) theoretical calculations, (b) numerical simulations, (c) background studies of natural changes similar to those hypothesized for the modification experiment, and (d) analyses of actual experiments. Each method has significant limitations. For instance, exact numerical simulations are not possible because of computer size limitations (which require assumptions for the solution of mathematical equations) and the inability to describe detailed storm structure and incorporate initial data in the models. Furthermore, hurricanes vary widely in structure, and the natural variability of a given hurricane is often of the same magnitude as the changes expected from the modification experiments. Thus the assessment of the possible changes that might be expected from a modification experiment, through the techniques listed above, is often more qualitative than quantitative. Nevertheless, until more experiments are carried out, these techniques provide the only

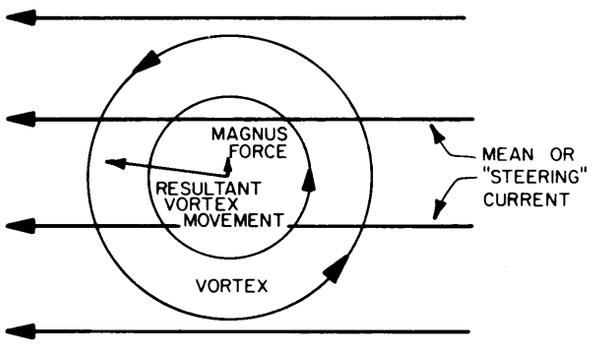

Figure 8.--Forces acting on a vortex embedded in a translational current.

information on possible impacts of Stormfury-type experiments on future storm structure and behavior.

3.1 Possible Effects on Track

The dominant influence on the motion of a hurricane is the surrounding large-scale flow in which the hurricane is embedded. This flow is often referred to as the steering current or advection and is the primary consideration in forecasting storm motion. Another factor contributing to the motion of the storm is the interaction of the vortex with the environmental flow, including asymmetric heating.

Kuo (1969) performed theoretical calculations that indicated under specified conditions that "the net pressure exerted by the fluid on the vortex core is made up of two parts: a lift or rotor or Magnus force...directed to the right or left of the current according to whether [the circulation] is positive or negative, and a residual Coriolis force. The motion under such circumstances is a steering motion by the mean current plus a trochoidal oscillation about the mean path...." The primary forces and resultant motion are illustrated schematically in fig. 8.

Jones (1977) conducted some numerical experiments on an f-plane and found good agreement with Kuo's theoretical calculations. Figure 9 shows the

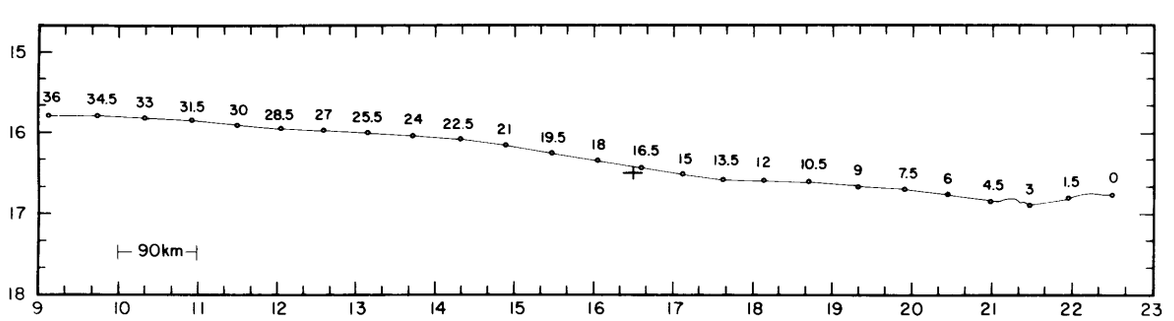

Figure 9.--Simulated track of vortex center for 10 m s^{-1} current. Numbers along track give time elapsed, in hours (Jones, 1977). Axis numbers identify grid points.

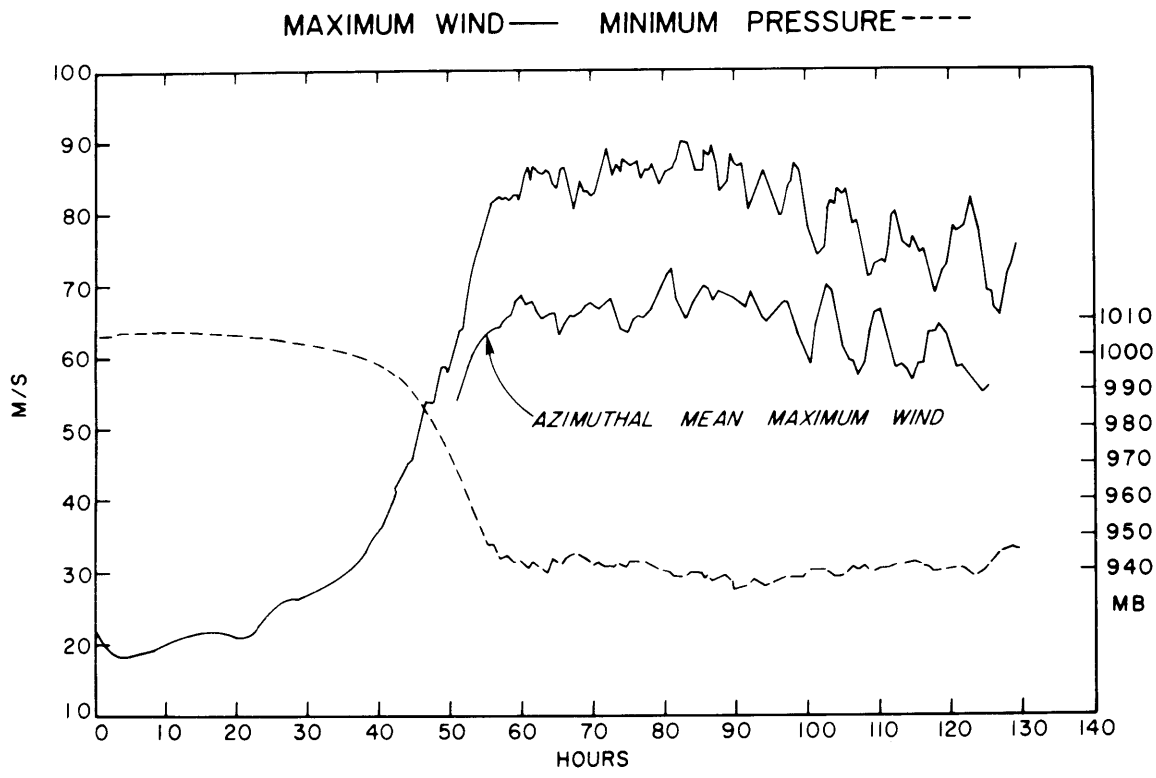

Figure 10.--Maximum low-level wind and minimum surface pressure for control experiment with moving 90-km grid (Jones, 1976).

simulated track of a model storm initially embedded in a mean easterly current of 10 m s^{-1}. At 18 h in the experiment, the uniform basic current at distances greater than 500 km from the center of the vortex was from approximately 92° at 9.4 m s^{-1}. The mean vortex velocity was 277° at 9.28 m s^{-1}. That is, the motion of the vortex was 5° to the right of the mean current and 0.12 m s^{-1} slower. Thus approximately 90% of the vortex motion in that experiment can be attributed to the mean current, and the remainder of the motion results from other vortex and mean current interactions.

Jones (1976) conducted experiments with a three-level, three-dimensional model of a tropical cyclone, enhancing the convective heating rate of a storm the way a modification experiment might, to study the motion of a modified storm versus the motion of a control case. Figure 10 shows the development, in time, of the model storm. The storm reaches a nearly steady state of 85 m s^{-1} winds and a minimum sea level pressure of 940 mb after about 60 h.

Figures 11 and 12 show Jones's modified tracks (and the control track) for artificial heating rates of about 1.3° to 1.7°C h^{-1} applied at the middle and upper troposphere (normal seeding simulation) and extreme heating (four times normal seeding simulation). This set of experiments was conducted on a 10-, 30-, and 90-km nested grid where the higher resolution grids moved on a fixed 90-km grid with the vortex initially embedded in a 5 m s^{-1} easterly current. Both seeding simulations began at 57 h into the experiment. The symmetric heating was applied for a total period of 10 h. The extreme heating (four times normal) was applied in an asymmetric fashion over a 21-h period. The results indicate small oscillations about the control track. Jones

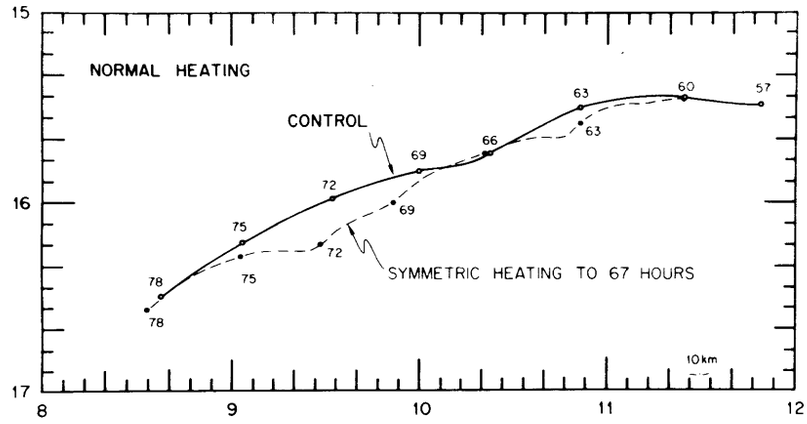

Figure 11.--Modified track for symmetric normal heating to 67 h compared with control. Numbers along track give time elapsed, in hours (Jones, 1976). Axis numbers identify grid points.

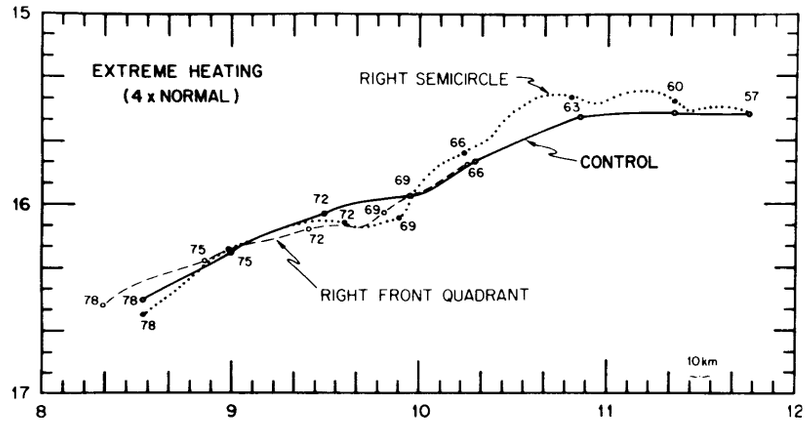

Figure 12.--Modified tracks for extreme asymmetric heating to 78 h compared with control. Numbers along track give time elapsed, in hours (Jones, 1976). Axis numbers identify grid points.

states that systematic deviations of the seeded tracks from the control-case track fall in the 1% to 3% range of the displacement of the storm, with the 1% value for the normal heating rate in the right front quadrant (a location similar to the seeding location of the present Stormfury experiment design).

Figure 13 shows results for symmetric heating carried out with a method similar to that described above, but on a moving 90-km grid. Significant oscillations from a track, smoothed over a period of several hours, can be seen in all tracks, including the control case, beginning after about 96 h. The seeded cases started to show some systematic deviations from the control case after about 110 h (about 36 h after seeding). Jones states that "the changes of the seeded tracks...seem to be related to changes of the relative location of the upper-level cyclonic circulation center with respect to the middle- and low-level centers...." That is, these centers were not vertically aligned. Jones attributed much of this deviation to model constraints, such

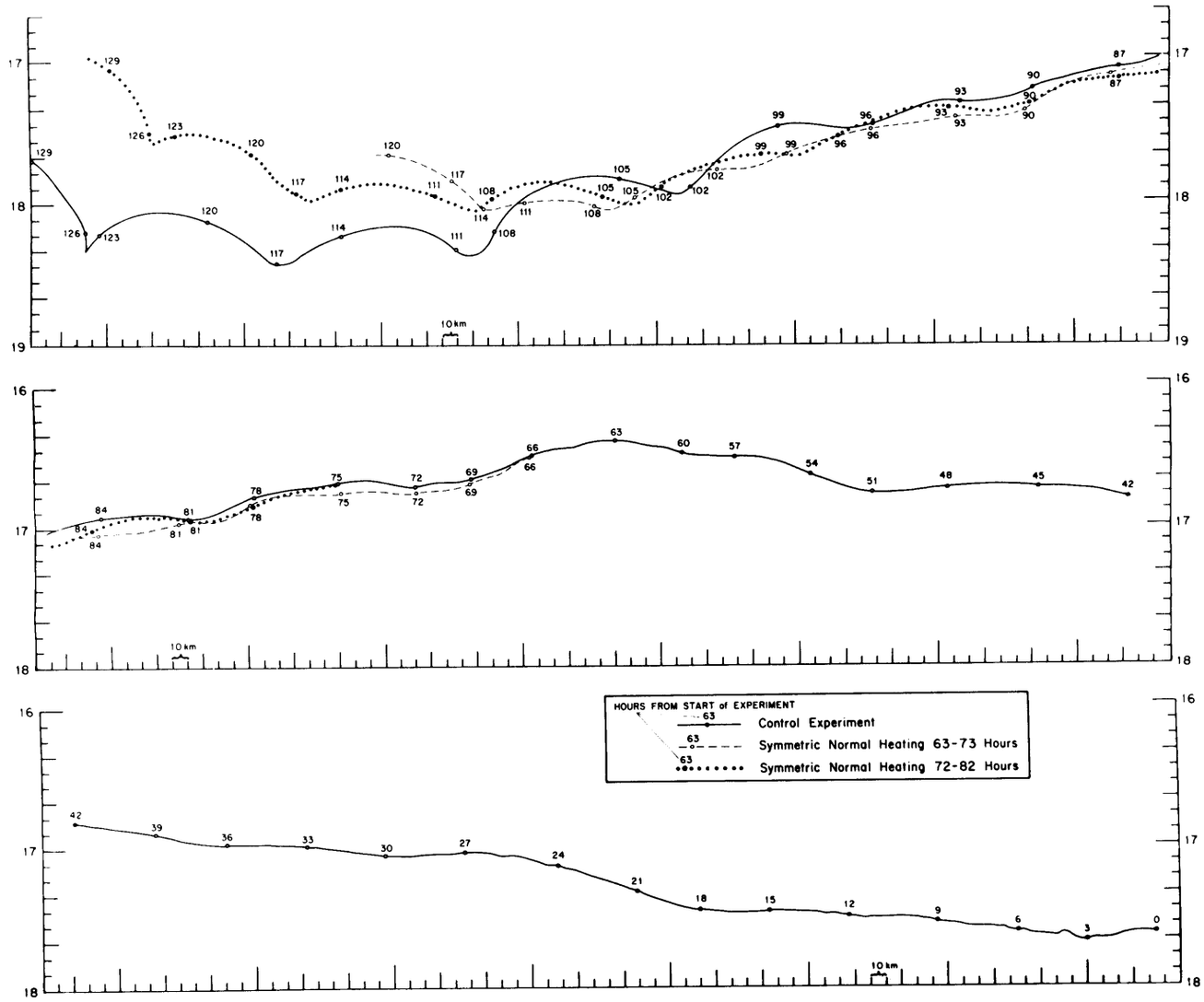

Figure 13.--Modified tracks for symmetric normal heating compared with control, on moving 90-km grid. Numbers along track give time elapsed, in hours (Jones, 1976). Axis numbers identify grid points.

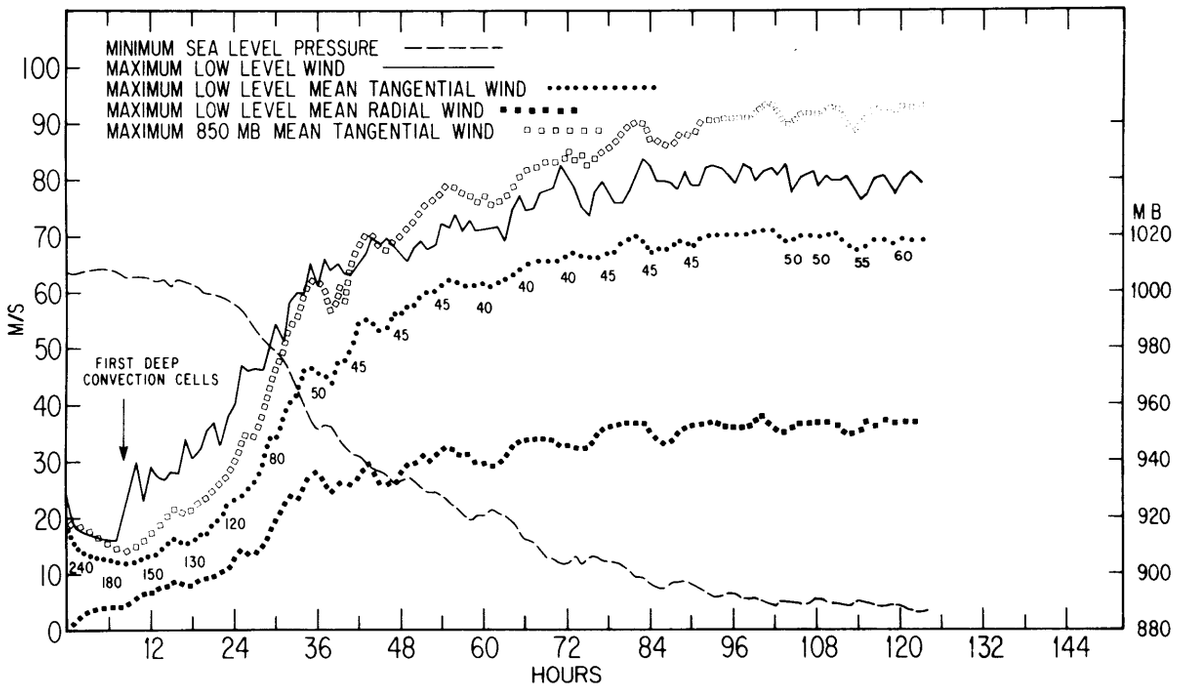

Figure 14.--Storm characteristics as developed in Jones's 12-level model.

as limited vertical resolution. He states that inclusion of "a parameterization of the vertical transports of horizontal momentum by cumulus clouds into the model...[should result in] much smaller mean track deviations...during the second day after seeding."

Jones recently ran experiments similar to those described above (but omitting the seeding) using a new 12-level version of his three-dimensional model. This model not only contains improved vertical resolution but also improved release of latent heat, etc. The preliminary results of these experiments are shown in figs. 14 and 15. Figure 14 shows the development of the storm; windspeeds reach a maximum near 90 m s^{-1}, and sea level pressure reaches a minimum of about 900 mb at about 72 h. The storm continues in a nearly steady state through 108 h. These conditions are rather extreme, with the minimum pressure being about 40 mb less than for the three-level-model experiments. However, the resultant motion, shown in fig. 15, is of particular interest for this study. This storm was initially embedded in a 5 m s^{-1} easterly current, as was the storm for the three-level experiment. Important features of these results are the considerably decreased amplitudes of the oscillatory motion for this case, compared with the three-level case, and the movement of the storm on a west, or slightly north-of-west, course, which became almost due west after 77 h; the three-level-model results showed a south-of-west course after 63 h. The amplitudes of the oscillations during the 80- to 90-h period are about 5 km and decrease to almost zero after 100 h. Compared with the amplifying situation for the three-level experiments, this result seems to support Jones's earlier conclusions that the amplifying oscillations in the three-level-model results were probably primarily caused by poor vertical resolution.

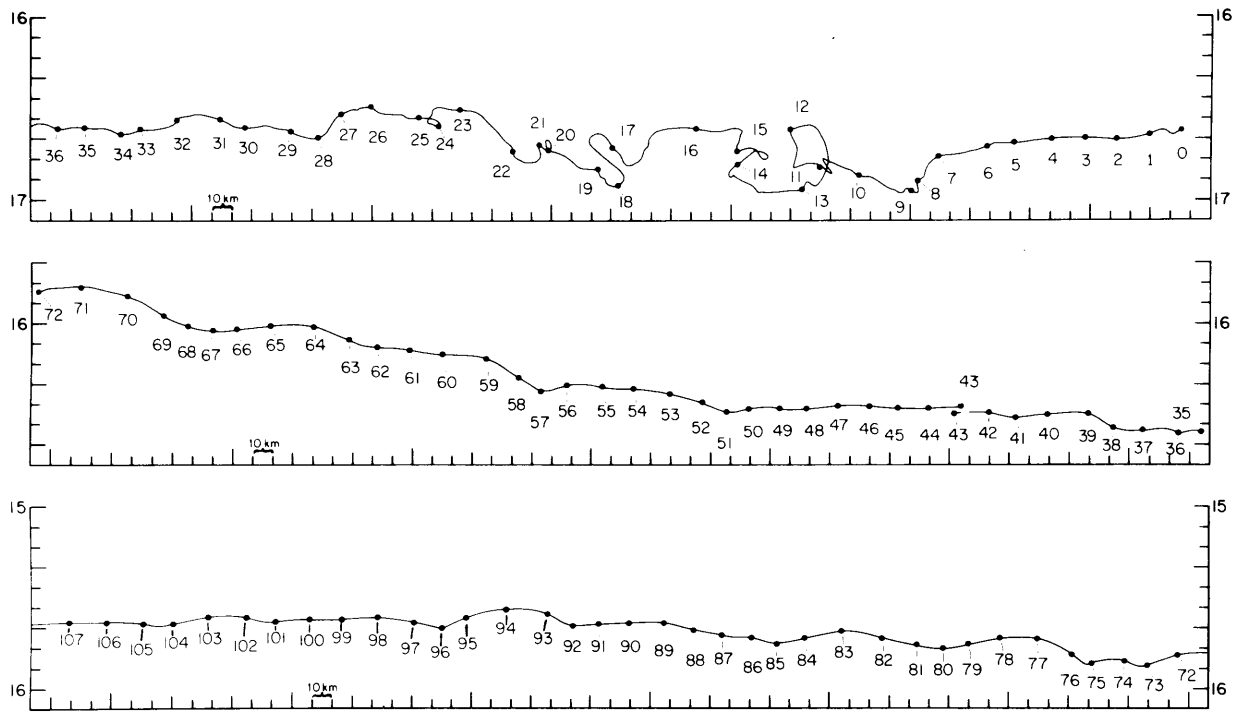

Figure 15.--Motion of model storm in fig. 14. Storm was initially embedded in 5 m s^{-1} easterly current. Axis numbers identify grid points.

George (1975) conducted observational studies in which tropical-cyclone motion was compared with surrounding flow. He used rawinsonde data collected from 30 stations in the western Pacific in the vicinity of tropical cyclones over 10 yr. Approximately 200 typhoons and 20,000 rawinsonde reports were included in the sample. These data were composited relative to the direction of storm motion and then stratified in several ways. Of particular interest is the comparison of storm motion and environmental flow with stratifications by intensity and speed of movement. Table 4 summarizes several stratifications. The data indicate that the storms generally moved to the left and slightly faster than the surrounding flow as determined through averages of the wind in annular rings from a radius of 1° to 7° from the center of circulation. The results for the case where the winds were averaged over the annular ring and integrated through a depth of 1000 to 500 mb indicate an average storm track deflection of about 16° to the left and storm movement that was 1.16 times faster than the mean flow. Figure 16 depicts these data in graphs.

These results are inconsistent with both the theory and the numerical simulations described earlier. A possible reason for this inconsistency is the way in which the mean circulation was determined. Specifically, George indicated that inclusion of upper-level data in the composites created considerable scatter. The lower-level data were very consistent, with little scatter and a high degree of correlation to the storm movement. However, the author states the aspect of the study important to this paper as follows: "the surrounding flow dictates the storm motion very well, regardless of

Table 4.--Vertical multiple radial band summary for 1° to 7° band*

Stratification of data	Mean storm direction (degrees)	Mean 1°-7° surrounding wind direction at 700-500 mb (degrees)	Storm deviation from surrounding wind (degrees to left)	Mean storm speed (m s^{-1})	Mean 1°-7° surrounding windspeed at 1000-500 mb (m s^{-1})	Ratio storm speed/ surrounding 1°-7° windspeed at 700 mb
Latitude						
> 20°N	352	007	15	5.61	4.55	1.23
< 20°N	300	312	12	5.05	4.05	1.25
Speed						
Slow storm (Speed 0-3 m s^{-1})	338	359	21	2.43	1.91	1.27
Moderate storm (Speed 3-7 m s^{-1})	326	342	16	5.19	4.03	1.28
Fast storm (Speed >7 m s^{-1})	006	017	11	10.12	7.77	1.30
Direction						
Direction A (250°<dir.≤310°)	285	302	17	6.16	4.65	1.32
Direction B (310°<dir.≤350°)	324	337	13	5.32	4.25	1.25
Direction C (350°<dir.≤060°)	027	040	13	7.08	5.67	1.25
Intensity						
Intensity 1 (1000 mb≥C.P.>980 mb)	319	333	14	4.87	3.71	1.31
Intensity 2 (980 mb≥C.P.>950 mb)	326	344	18	5.03	3.87	1.29
Intensity 3 (C.P.≤950 mb)	319	340	21	5.17	4.08	1.28
Intensity change						
Deepening storms	304	318	14	4.89	3.82	1.28
Filling storms	360	019	19	5.69	4.55	1.25
		Mean:	15.7°		Mean:	1.27
		Standard deviation:	3.3°		Standard deviation:	0.03

*George (1975)

storm latitude, speed, direction [of movement], intensity, and intensity change. Thus, it appears that the structure of tropical cyclones such as the inner convective activity is not a primary factor in influencing storm movement."

Another way of addressing the question of whether seeding might cause large and/or systematic changes in the storm track is to examine the results of actual seeding experiments. A study of the tracks of the four storms seeded under this program was conducted using the official forecasts of the National Hurricane Center (NHC) and the objective NHC CLIPER (CLImatology and

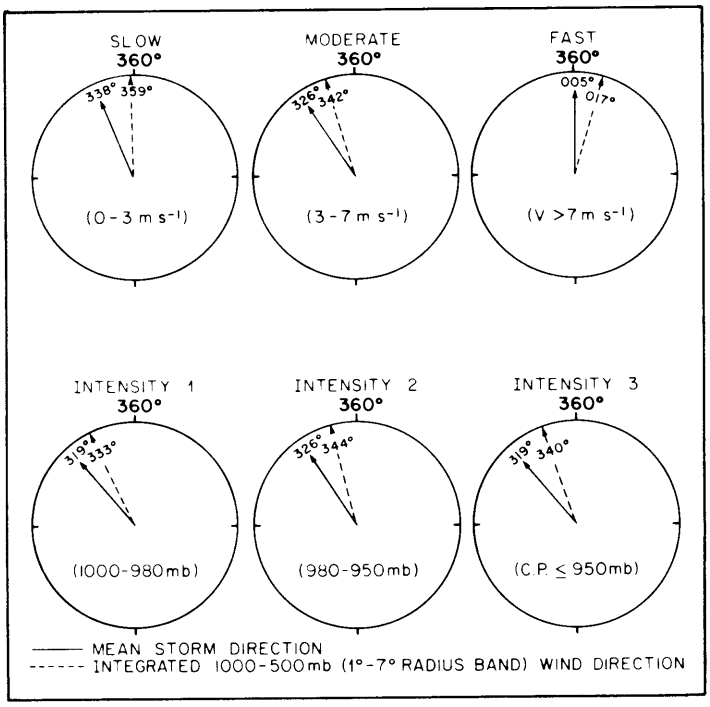

Figure 16.--Relationship between the mean storm direction and the surrounding wind flow for speed and intensity stratifications (vertical multiple radial band) between 1000 and 500 mb and 1° to 7° radius (George, 1975).

PERsistence) system (Neumann, 1972) to compare the expected movement of the seeded storms with the actual movement. Although the sample is small, no obvious changes caused by seeding were detected. Details of the results of this study are given in Appendix A.

The number of cases and the detail of data available for study make it impossible to determine with certainty whether the motion of the storm is affected in some small way by seeding. However, the following indications are clear:

(1) Storm motion is primarily determined by the large-scale flow (steering current) in which the storm is embedded and it is highly unlikely that Stormfury-type seeding experiments (seeding conducted relatively close to the center of the storm) would have any detectable and/or significant effect on this large-scale component of motion.

(2) No effect on storm motion has ever been detected in past seeding experiments.

(3) Any changes in motion that might occur as the result of seeding would probably be quite small, less than the diameter of the eye, not systematic, and difficult to detect because of the natural variability of storm motion.

Table 5.--Computed and assumed precipitation around a hurricane-typhoon based on Atlantic and Northwest Pacific data stratified by degrees-of-latitude rings centered on the storm*

Radius (deg.lat.)	0-2	2-4	4-6	6-8	8-10	10-12
Precipitation (cm d^{-1})	9.0	2.3	0.7	0.7	0.7	0.7

*Frank (1976)

3.2 Possible Effects on Rainfall

All studies on tropical-cyclone-produced rainfall have indicated large rainfall variabilities (rates as high as 50 cm d^{-1} to as low as 1.5 cm d^{-1}) with little or no correlation to storm intensity (Miller, 1958; Schoner and Molansky, 1956; Brunt, 1966; Milton, 1978).

Frank (1976) computed mean rainfall rates and totals for tropical cyclones using composited data from both the Atlantic and Northwest Pacific. The results of his study indicated that approximately 75% of the total precipitation within 12° of the storm center occurred at a radial distance greater than 2° from the center (table 5). However, the rain rates beyond 4° to 6° radial distance were not much different from seasonal averages.

Frank's calculations also indicated that approximately 75% of the precipitation that occurred in the 0° to 2° ring resulted from an inward advection of water vapor as opposed to evaporation from the sea surface in this region. This advection should not be affected appreciably by the magnitude of changes anticipated in the inner core. Therefore, the total water vapor available for precipitation should remain nearly unchanged as a result of the modification of the inner convection of the tropical cyclone.

A study by Griffith et al. (1978) noted large variations in rainfall from storm to storm. The authors concluded that "there is no relationship between storm intensity and either volumetric rain output or average rain depth." Their statistics for the limited number of cases presented also indicate that a given storm tends to be wet or dry and not to change much with time or to correlate with intensity changes. Details of this study are given in Appendix B.

Simulated seeding experiments by Rosenthal (1971) and Rodenthal and Moss (1971) indicated the diversion of boundary layer inflow and the formation of a new eyewall 10 km radially outward from the original. The rainfall rates obtained from these experiments are illustrated in fig. 17. The experiment results indicate an increase in rainfall rate near the end of the seeding period with little net change at any other time. An outward shift of the location of maximum rainfall rate, reflecting the outward shift of the eyewall, is indicated although a high degree of temporal variability was observed.

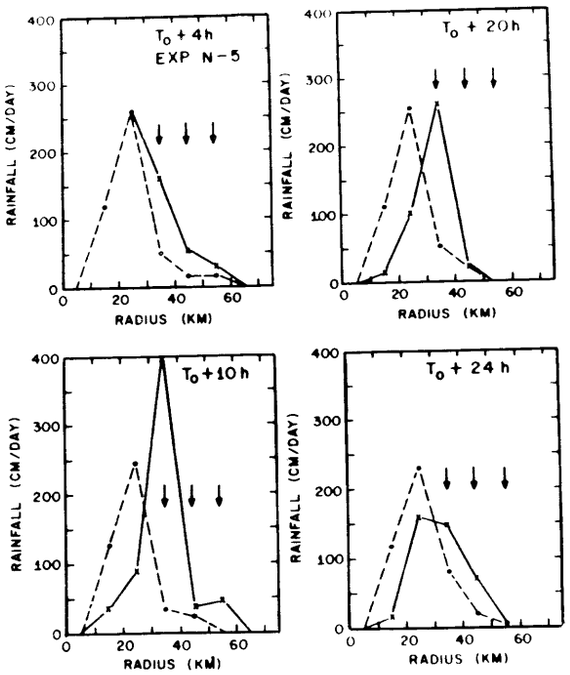

Figure 17.--Computed rainfall rate results from a control (dashed line) and a seeding (solid line) experiment where artificial heating is applied from hour 288 (T_0) to hour 298 at radii of 35, 45, and 55 km (arrows) (Rosenthal and Moss, 1971).

Jones (1976) performed calculations with heating rates comparable with the two-dimensional experiments using a three-level, three-dimensional model. Although Jones's experiments "were not as successful in reducing the maximum wind as were the symmetric model seeding simulations of Rosenthal and Moss (1971)," the computed rainfall rates from these experiments (fig. 18) do not differ greatly from the instantaneous two-dimensional results illustrated earlier. There is an outward shift at 90 h, but little deviation from the control at 108 h. In both of the two- and three-dimensional simulations, net rainfall amounts in the control and modified cases differ little.

In another study, Sheets and Knight simulated the effect of hypothetical changes on the total precipitation and the precipitation distribution as a typical storm passed over an area (see Appendix C). The initial eyewall was assumed to nearly dissipate, whereas the seeded area was assumed to increase in rainfall rate, and the storm was assumed to move at 5 m s^{-1}. No statistically significant changes were observed in the cumulative rainfall over the storm area, and cumulative point totals seldom varied by more than 10% as a result of the simulated modification.

The Stormfury hypothesis assumes that modification of the central core of a mature hurricane will reduce the maximum windspeeds. The modification primarily consists of a redistribution of the location of the major vertical mass transport near the storm's center. It is assumed that such a redistribution does not appreciably affect cumulative rainfall areawise or pointwise. This assumption is based on the following conclusions from the studies described:

(1) The amount of rainfall produced by tropical cyclones varies considerably from storm to storm.

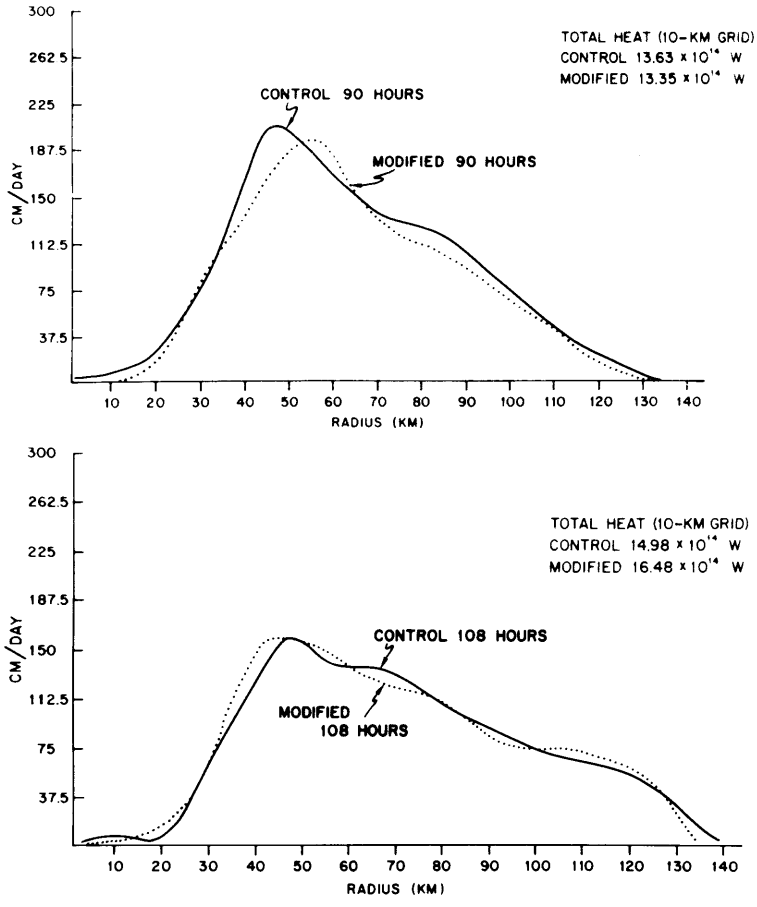

Figure 18.--Azimuthal mean rainfall rates for modified (symmetric normal heating, hour 72 to hour 82) and control experiments on moving 90-km grid. All times are given in terms of hours into the experiment; i.e., data in top figure are for time 8 h after end of seeding (Jones, 1976).

(2) The amount of rainfall generated by a given tropical cyclone appears to be primarily a function of large-scale features in which the cyclone is embedded, or at least it has no significant correlation with its intensity.

(3) Alterations of the rainfall pattern near the center of the storm (the only area where Stormfury-type experiments are hypothesized to have an effect) will, in all likelihood, have little effect on the areawide, or point accumulations of rainfall for a moving storm.

3.3 Possible Effects on Wind Field

No increase in storm intensity is expected to occur from experiments based on the Stormfury hypothesis. Table 3 shows that in none of the experiments conducted to date was an increase in maximum windspeed observed. The most extensive data sets were collected for the two Debbie experiments where decreases in windspeed were observed over the entire central portion (inner 100-km radius) of the hurricane. These changes were well documented (Gentry,

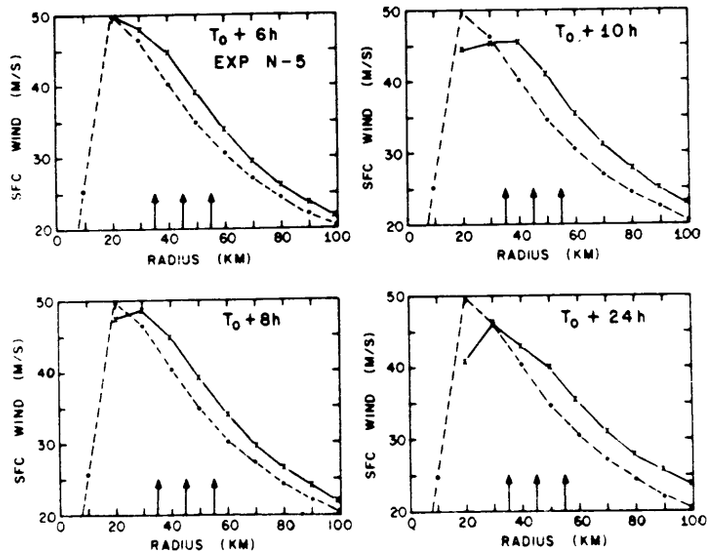

Figure 19.--Surface wind field results from a seeding experiment where artificial heating is applied from hour 288 (T_0) to hour 298 at radii of 35, 45, and 55 km. Dashed line is control case; solid line is seeding case with arrows showing seeding locations (Rosenthal and Moss, 1971).

1970; Hawkins, 1971; Sheets, 1973). One area that did not receive extensive monitoring was the region farther than about 100 km from the storm center.

Numerical simulations by Rosenthal and Moss (1971) made with a circularly symmetric model indicate that windspeeds could be reduced near the storm center by experiments conducted in a manner similar to that prescribed by the Stormfury hypothesis, but that windspeeds should increase in the region just outside the original radius of maximum wind. Figure 19 shows maximum increase located around 60 km (about twice the original radius of maximum winds) and only minor increases noted at radii greater than 70 to 80 km. Rosenthal and Moss (1971) state, "It is the increased centrifugal and coriolis forces arising from these larger winds that prevents the inflow from reaching the original eyewall and thus forces ascent at a larger radius." That is, in this model, you cannot get a decrease of maximum winds without getting the increase in winds at larger radii. However, Rosenthal (1971) cautions that "results obtained from the model must not be taken too literally. We do not contend that the model conditions are found in the real atmosphere.... At best, the results should be considered qualitative guidance material." Of course these statements are applicable to all the model results, including the reduction in windspeed as well as the increase at the larger radii.

Hawkins (1971) presented several wind profiles observed before, during, and after the Hurricane Debbie experiments. The distinct trend was a decrease in windspeed over the entire region sampled within 100 km of the storm center for the majority of the cases (figs. 20 and 21). Hawkins pointed out the large natural variability between profiles for a given azimuth, as well as for different azimuths from the storm center. In presenting the only two wind profiles recorded that extend well away from the storm center for the two Debbie seeding experiments (figs. 22 and 23), he cautioned that there were variations in the azimuth over which the data were collected, and that the

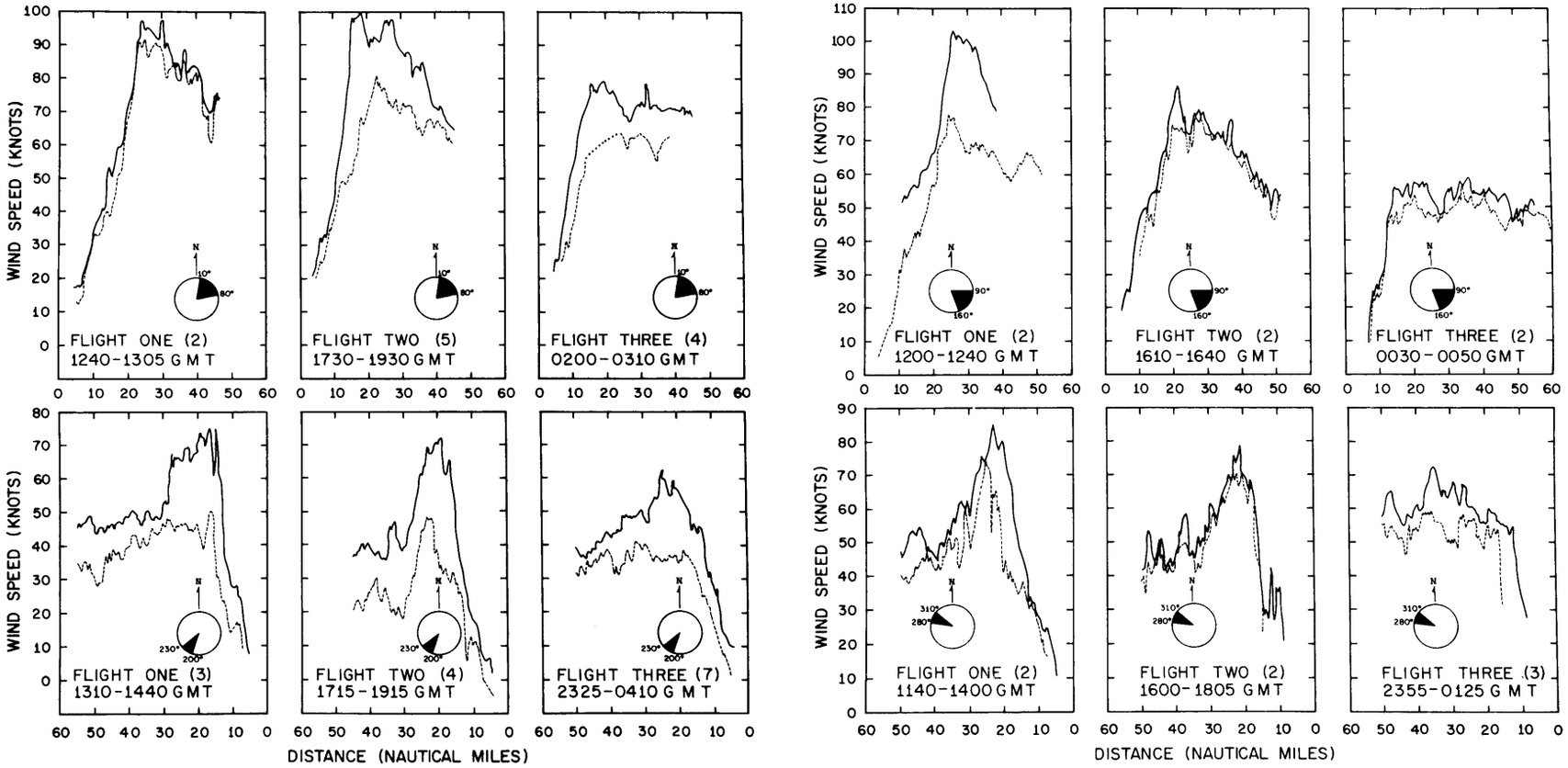

Figure 20.--Windspeed envelopes (at 12,000 ft) for August 18 (left) and 19 (right) showing the maximum and minimum windspeeds at the indicated radial distance for the available number of radial passes (noted in parentheses). The profiles are segregated according to azimuth angle relative to the storm center. The left panels depict preseeding conditions, the central panels are roughly from midseeding conditions, and the right panels show postseeding envelopes (Hawkins, 1971).

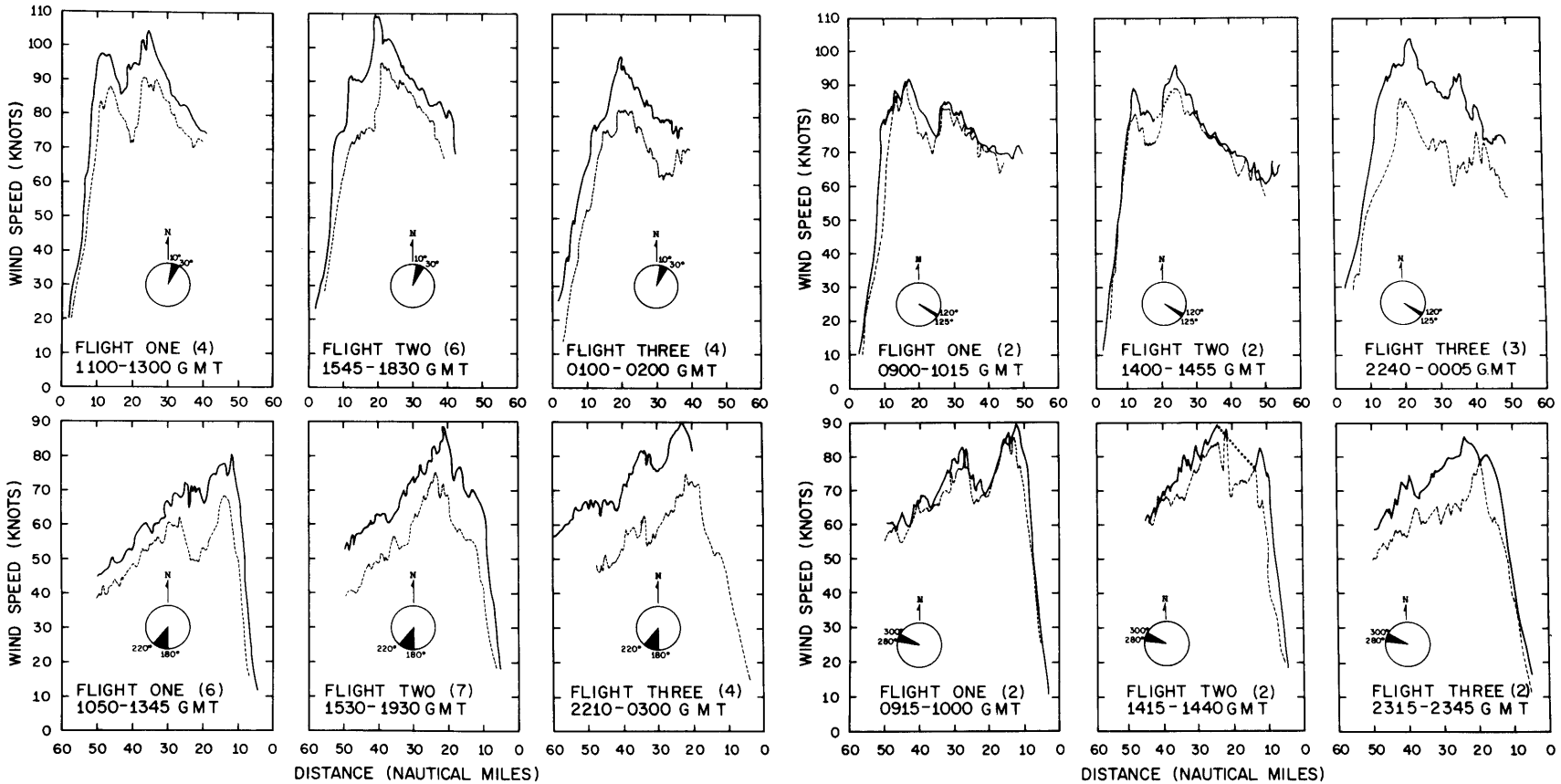

Figure 21.--Windspeed envelopes (at 12,000 ft) for August 20 (left) and 21 (right) (Hawkins 1971); see legend for fig. 20.

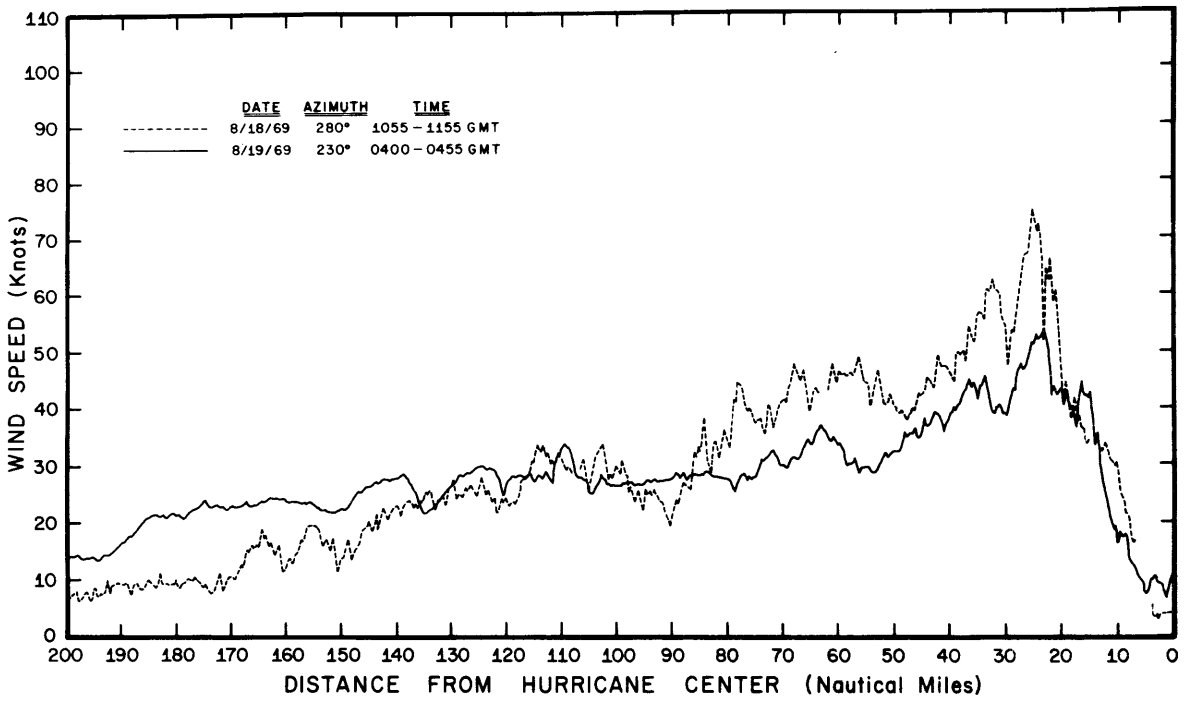

Figure 22.--Windspeed profiles (12,000 ft) from the original approach to Hurricane Debbie on August 18, before the seeding with silver iodide, and the final exit on August 19, long after the seeding (Hawkins, 1971).

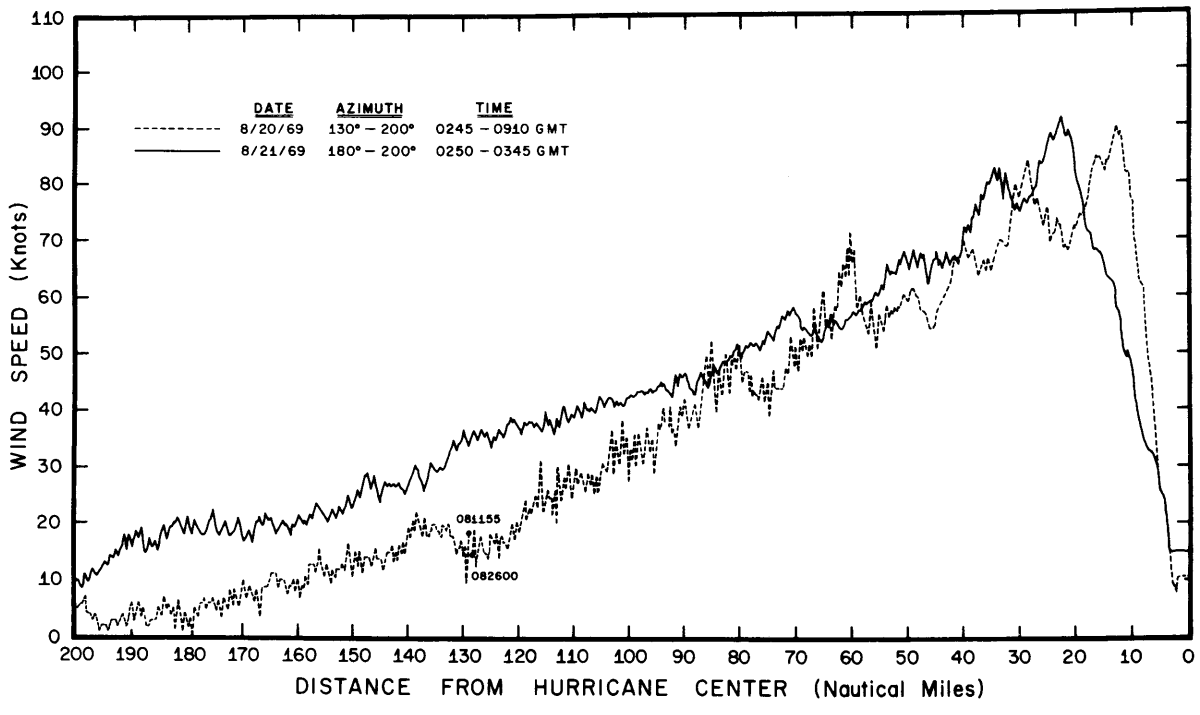

Figure 23.--Windspeed profiles (12,000 ft) from the original approach to Hurricane Debbie on August 20 and the final exit on August 21. On the approach, the aircraft did not reach a 12,000-ft altitude until reaching the 175-nmi radius, but was above 8000 ft when passing 200 nmi (Hawkins, 1971).

infrequent sampling might not be entirely representative "to characterize the strength and structure of a storm ...[and it] can be misleading." Also, whether the increases in windspeeds shown at large distances from the storm center for the Debbie cases are representative is unknown. In any case, a question remains about the possibility that a detectable and/or significant increase in windspeed away from the original radius of maximum wind would result from seeding.

Thus, both past experiments and numerical simulations indicate that the maximum windspeed should be reduced when Stormfury-type experiments are conducted. Some questions remain concerning the winds outside the radius of maximum winds. However, it appears that increases, if they do occur, would be small and would not significantly contribute to increases in damage since they would probably be confined to regions where windspeeds are not dangerously high before seeding. Verification or repudiation of this postulated structure will have to await further experimentation and observations of natural storm variabilities.

3.4 Possible Effects on Storm Surge

The effect of tropical cyclone modification on storm surge is difficult to assess because storm surges vary widely. The magnitude and extent of storm surge depend primarily on two factors:

(1) Strength and length of fetch (duration and strength of onshore winds).

(2) Bottom topography. (For example, a gently sloping continental shelf will experience a larger storm surge than a steeper shelf.)

The surface pressure field of a tropical cyclone contributes to the height of the storm surge primarily through the generated wind fields. The pressure differential is of secondary importance because of the differences in the density of air and water. For example, if the standard atmospheric pressure at the surface (1013 mb) were reduced by about one-tenth, the resulting surface pressure would be about 912 mb, which would represent an extreme

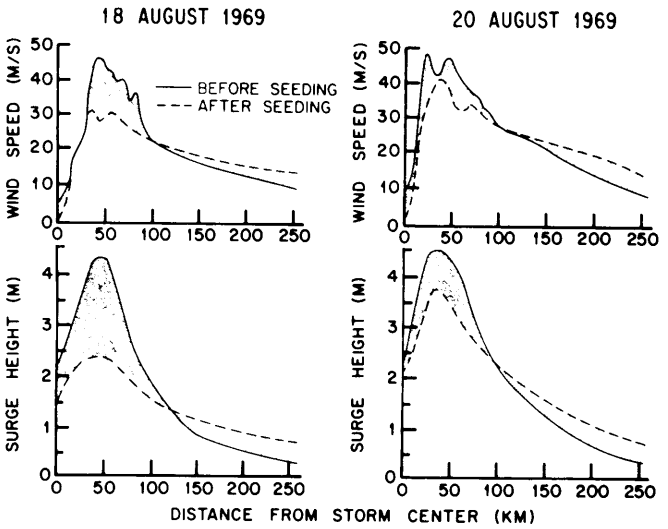

Figure 24.--Profiles of observed windspeed and computed open coast surge for Hurricane Debbie (1969) (Jelesnianski and Taylor, 1973).

hurricane case with a strength near that of Camille (in 1969) (Simpson et al., 1970). The compensating rise in the level of the ocean surface to offset this decrease in atmospheric pressure would be only ~1 m, compared with a peak surge for Hurricane Camille of ~8 m. The strength and length of fetch depend on the strength and extent of the high-wind area and the direction and speed of storm movement. Variations of any of these factors and/or the bottom topography and coastline configuration result in large changes in the generated storm surge.

Jelesnianski and Taylor (1973) conducted a series of experiments with their SPLASH model to assess storm surge and wind field relationships. They also applied the SPLASH model to the Hurricane Debbie (1969) case for wind profiles measured before and after seeding on August 18 and 20 (fig. 24). The results indicate that the maximum surge could have been reduced by as much as 2 m on August 18 and 0.75 m on August 20, with substantial reductions over the region from the center of the storm to a radial distance of 90 to 100 km (50 to 60 nmi). At larger radial distances, the peak surge increased by 0.3 to 0.4 m as a result of the input of increased windspeeds at these radii.

Jelesnianski and Taylor concluded that a reduction in the maximum wind did not necessarily result in a reduction in the peak surge. Simulation of such a modification is illustrated in fig. 25. The 1979 SPLASH model was run

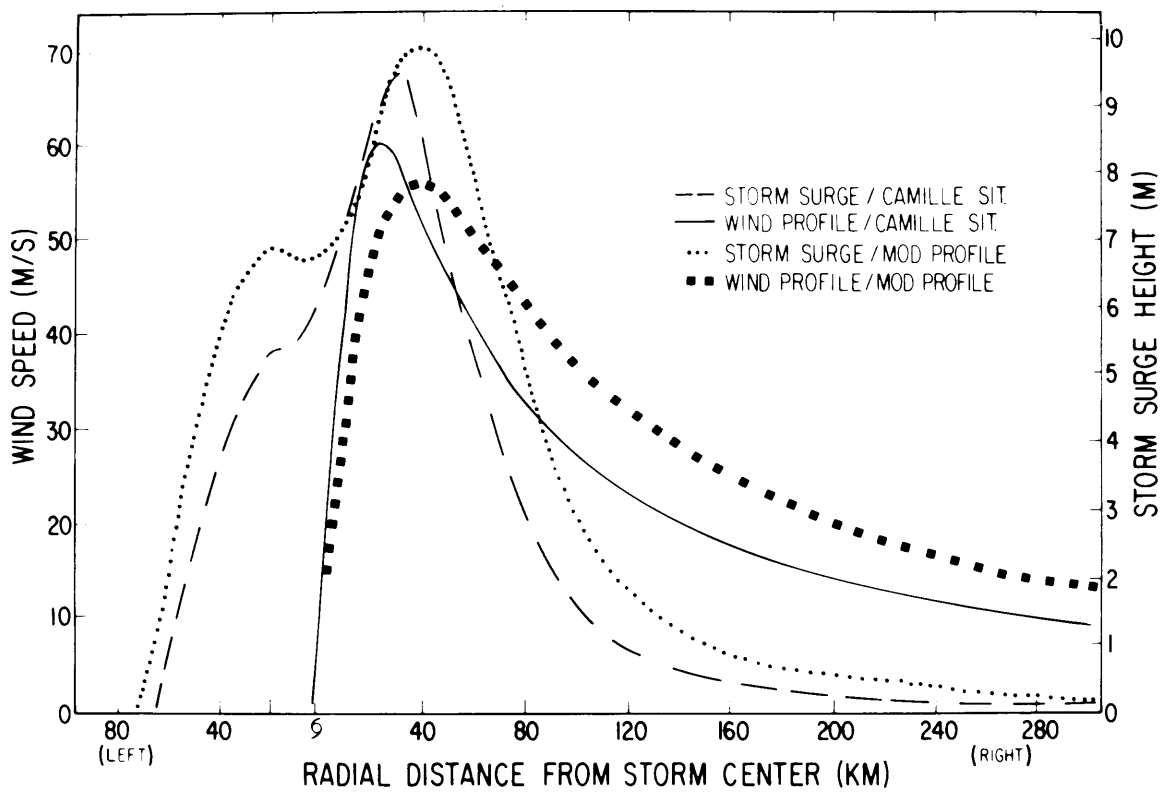

Figure 25.--Storm surge as simulated with 1979 SPLASH model: Camille (1979) situation in which RMW = 15 mi, maximum winds ~60 m s^{-1}, movement = 12 kn NNW, and ΔP = 100 mb; modified situation in which RMW = 24 mi, maximum windspeed ~55 m s^{-1}, and the values for movement and ΔP are the same as the Camille situation.

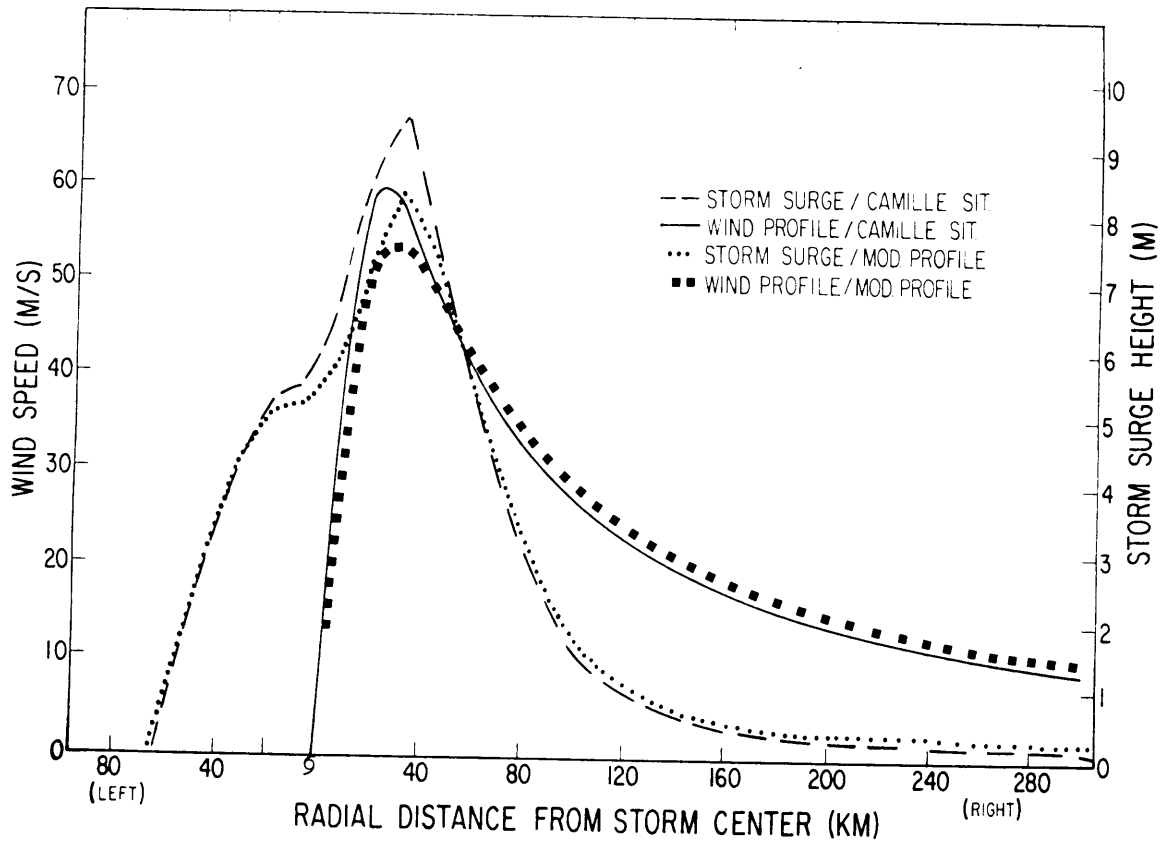

Figure 26.--Storm surge as simulated with 1979 SPLASH model: Camille (1979) situation (see legend for fig. 25); modified situation in which RMW = 18 mi, maximum windspeed ~53 m s^{-1}, ΔP = 85 mb, and movement is the same as the Camille situation.

for a Hurricane Camille (1969) situation along the gulf coast of the United States and was then modified by reducing the maximum wind by 5 m s^{-1} and shifting the radius of maximum winds outward to a radius of about 39 km. The pressure differential was held fixed at 100 mb. The computed windspeed profile shows significant increases almost everywhere at radii greater than the original radius of maximum winds. The storm surge increases despite the reduction in maximum winds. However, it increases only where the winds increase, all other things being equal. This condition may have little relevance to the hurricane modification as described earlier, since it is not in compliance with $V_\theta r^x$ = constant where x = 0.4 to 0.7, and increases in windspeed at the seeded or larger radii are in doubt.

Results of another, perhaps more realistic, simulation are shown in fig. 26. Again, the Camille situation is simulated. The modification consists of a wind profile change similar to that postulated under the Stormfury hypothesis, that is, a 10% reduction in windspeed accompanied by an increase in the radius of maximum winds to 1.2 times the original radius. (These two factors combine to give a value of $x \approx 0.6$ in the relationship $V_\theta r^x$ = constant as in fig. 4.) The result is that the storm surge decreases more than 1 m over the region of the maximum surge, and no significant change in storm surge occurs anywhere else. Greater reductions in the storm surge would result if we assumed 15% reductions in windspeeds with appropriate increases

in the radius of maximum wind. Note that a 15-mb reduction of the pressure differential was required to adjust the model wind profile to follow the relationship $V_\theta r^x$ = constant where $x \simeq 0.6$ for the peak wind reduction. As indicated, the pressure differential has little direct effect on the storm surge (a difference of about 15 cm for this case as compared with the unmodified case). The important factor is the windspeed profile. The major conclusion from the two simulated modifications is that, all other conditions being equal, the storm surge will not increase at any location unless the new wind at that location is increased.

The question remains of what would happen if windspeeds were increased at larger radii. However, the region within 100 km of the center point of landfall is where most of the damage occurs because of storm surge. A reduction of the magnitudes and areal extent indicated in the Debbie (1969) computations and the Camille simulation would result in a considerable reduction of damage for hurricanes making landfall. The increase at larger distances, if real, would probably have minimal impact for most areas, since an increase of the surge by about 0.3 to 0.4 m in these areas would result in a total surge averaging about 1 to 2 m.

4. EXPERIMENT DESIGN

The Stormfury experiment is designed to try to initiate the hypothesized modifications by seeding and to document the actual sequence of the hypothesized events. Both the seeding method and the ability to document changes in the storm structure have improved dramatically since the last Stormfury experiments were conducted (1971). Table 6 lists the present instrumentation on one of NOAA's P-3 aircraft for use in the Stormfury experiments. Such instrumentation has the capability to provide detailed documentation of the structures of both seeded and unmodified storms.

A frequency diagram of changes in maximum windspeeds for hurricanes of various intensities (fig. 27) illustrates that changes of 10% in 12-h periods are common. That is, the natural variability of hurricanes is of the same magnitude as the changes that are hypothesized to occur from seeding. This condition, then, requires nearly continuous monitoring over a period longer than 24 h to observe long-term trends, as compared with short-term oscillations, so that the sequence of events that may be associated with the seeding is documented. In addition, we would like to minimize natural fluctuations, such as interactions with land, upper level troughs, cold water, etc. For these reasons, a seeding candidate is ideally chosen as follows:

(1) The storm should be a mature tropical cyclone with a well-formed eyewall.

(2) The storm should be well away from large land masses and forecast to remain over favorable waters (warmer than 26.5°C) for at least 24 h after seeding.

(3) The storm should be forecast to remain under favorable synoptic flow conditions (not about to interact with an upper level trough or cold low that could significantly increase the vertical shear of the horizontal wind or cause recurvature) for at least 24 h after seeding.

(4) The storm should be forecast to remain within about 1300 km (about 700 nmi) of an operational base for at least 24 h.

Table 6.--Instrumentation available on NOAA P-3D (42RF) for Stormfury experiments

I. Sensors of Meteorological Parameters	
Temperature	Rosemount total temperature
Pressure	Static-dynamic, Garrett
Dewpoint	General Eastern
Sideslip	
Winds	Omega-INS TAS computed
Wind-temp.-humidity profile	Omega dropwindsonde
Vertical wind	High-resolution angle of attack pitch angle, vertical acceleration
II. Sensors of Cloud Physics Parameters	
Cloud droplet spectrum	PMS Knollenberg 2-D probe
Hydrometeor size spectrum	PMS Knollenberg 2-D probe
Small cloud droplet spectrum	FSSP forward-scattering probe
Hydrometeor size spectrum	Foil impactor (MRI)
Cloud liquid water	Johnson-Williams hot wire
Cloud particle structure	Formvar-DRI-cloud particle replicator
Icing rate	Rosemount icing rate meter
Ice particle	Knollenberg ice particle counter
Total integrated liquid water	Microwave radiometer
III. Sensors of Radiation	
Sea surface temperature	Barnes PRT 5
CO_2 air temperature	Barnes PRT 5
IV. Radar (digitized)	
C-band PPI lower fuselage 360° scan (horizontal) fan beam radar	
X-band RHI tail 360° scan (vertical) radar	
C-band PPI nose 240° scan conical	
V. Miscellaneous	
Airborne expendable bathythermograph launch mechanism	
Photography (nose, side, vertical)	
Automatic satellite data link	
Radar altimeter	
Seeder	
VI. Navigation	
Inertia navigation system	
Omega navigation system	
Doppler radar	

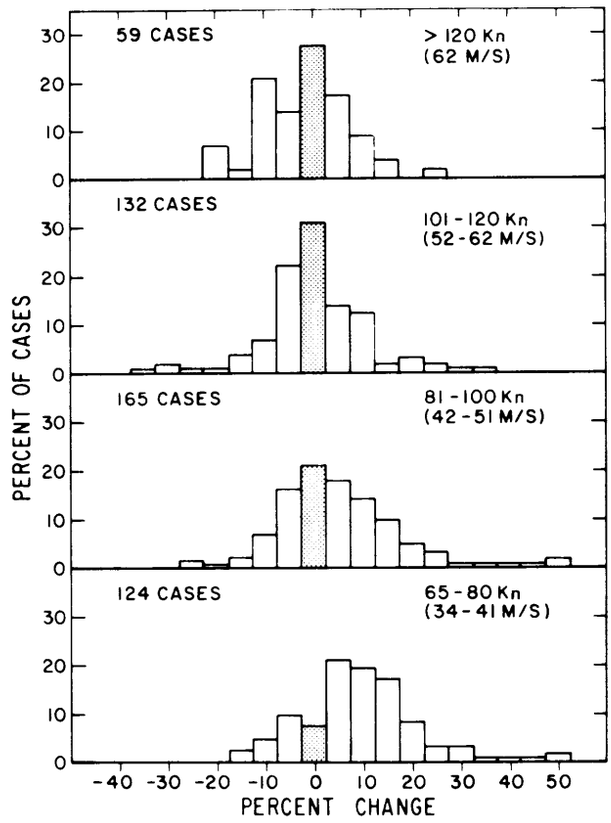

Figure 27.--Maximum windspeed 12-h changes, stratified by intensity, for Atlantic hurricanes from 1961 through 1968. Windspeeds were computed from minimum sea level pressures (after Sheets, 1970).

The current design of the experiments calls for five aircraft and seven crews. Representative flight patterns are illustrated in fig. 28, along with a typical seeding area. In comparison, the Hurricane Debbie experiments used 16 aircraft. However, these aircraft had very limited capabilities that were generally single purpose. For instance, the seeder aircraft could only seed. Middle- and upper-level aircraft had only limited meteorological measurement and recording capabilities and poor radars. Essentially, no cloud physics measurements were possible, and only qualitative radar observations were obtained. Present project aircraft have quantified, digitized radar systems for both horizontal and vertical sampling of the hurricane. Figure 29 illustrates the vertical radar (RHI) sampling capability. A vertical slice is obtained every 7 s as the aircraft passes back and forth through the storm. Composites of these data give detailed, three-dimensional depictions of the convective structure. This capability, coupled with the quantified horizontal (PPI) radar depictions, allows precise deliveries of the seeding agent. It also gives a thorough documentation of the storm structure and its changes. Other capabilities exist to document cloud physics elements, sea surface and subsurface temperatures, thermodynamic properties, and vertical distribution of winds as well as more standard 1-s horizontal profile measurements of wind, pressure, temperatures, humidity, vertical wind, etc.

Figure 30 shows the periods and levels of proposed monitoring and seeding. Each block represents a specific flight; typical flight patterns are

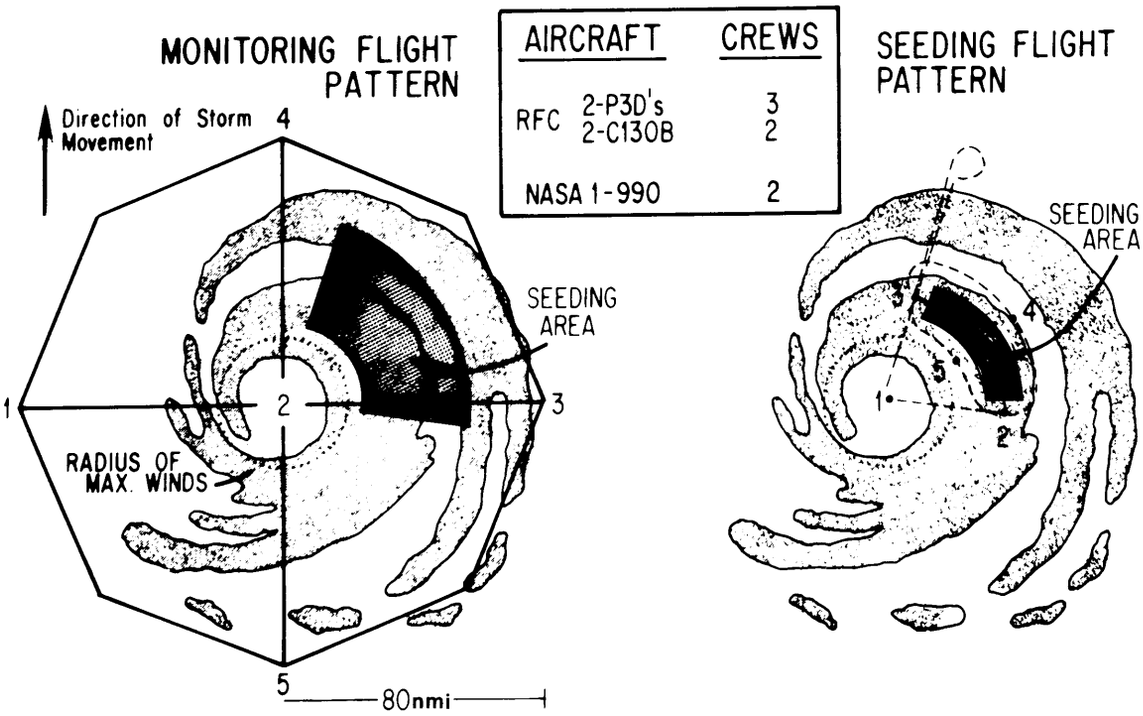

Figure 28.--Representative monitoring and seeding flight patterns for Stormfury experiments. Seeding-area location depends on availability of suitable clouds.

illustrated in miniature form above the block. For a single experiment, monitoring would be attempted through the total 58-h period; for a double experiment on a single storm (similar to the Debbie case), the sequence of flights would be stopped at the vertical dashed line and restarted for the second seeding about 44 h after the initial seeding began. This type of monitoring permits nearly continuous low-level windspeed and other basic meteorological parameter measurements, cloud microphysical measurements at the -5° to -15°C levels, and upper-level outflow characteristics before, during, and after seeding, along with nearly continuous data from quantitative range height indicator (RHI) and plan position indicator (PPI) radar. These data sets should permit an evaluation of the seeding based on physical reasoning from cause to effect, and a statistical analysis based on a randomization in time, response characteristics, and a sequence of events approach (Knight and Brier, 1978). Attempts will be made to document such factors as the existence of supercooled water, its conversion to ice, resultant cloud growth, relocation of the major region of vertical mass transport, air-sea interaction, and possible upper-level trough interaction.

The most difficult to document will be the cloud microphysical processes. These processes are not fully understood in the single-cloud situation and are even less understood in the hurricane environment. However, there is little doubt that major changes, such as cloud growth or dissipation, revealed by radar will be thoroughly documented. No significant change in intensity, wind field structure, convective structure including rainfall, storm motion, etc. should go undetected.

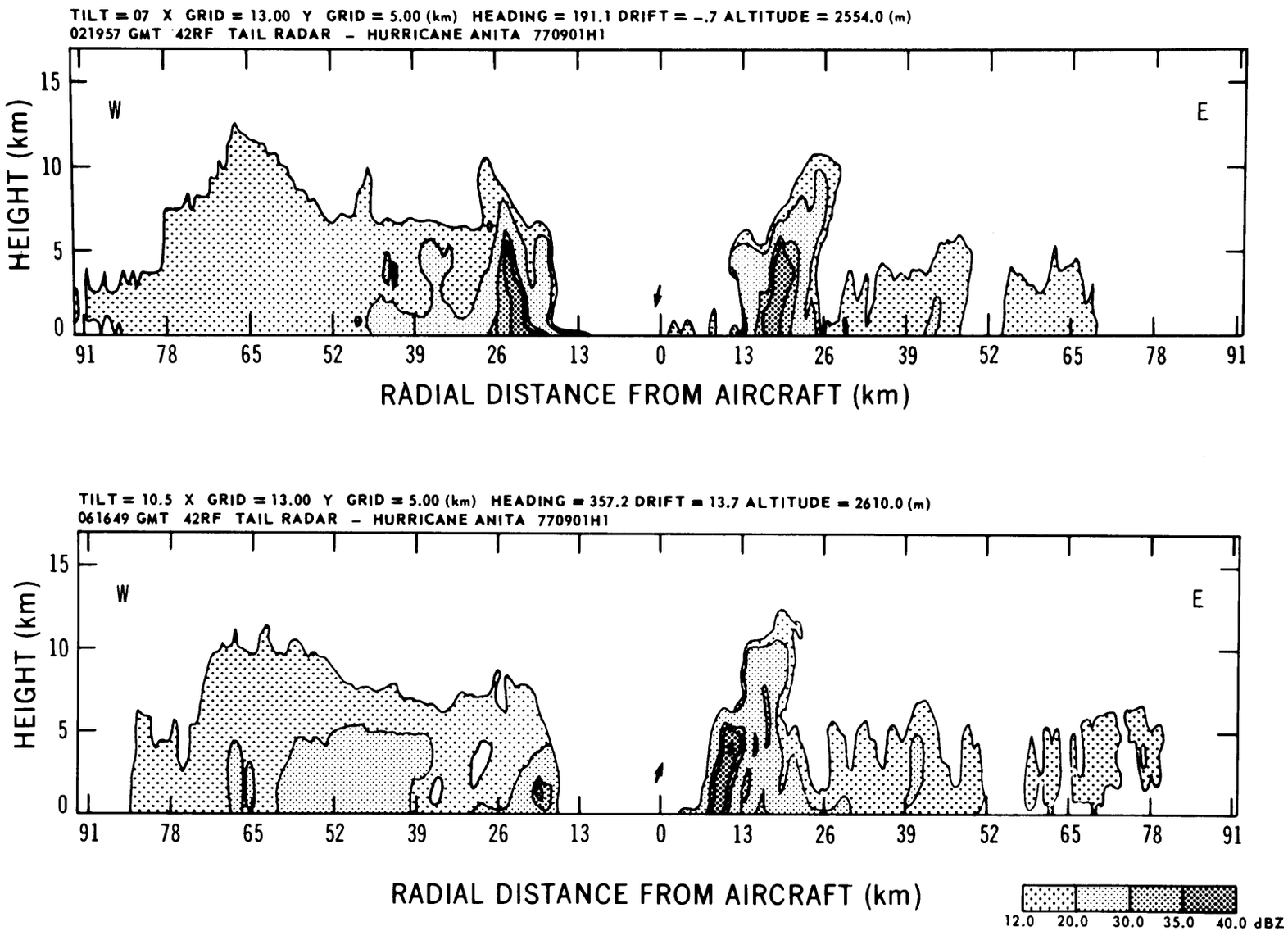

Figure 29.--Vertical radar cross sections through the eye and surrounding region of Hurricane Anita on September 2, 1977.

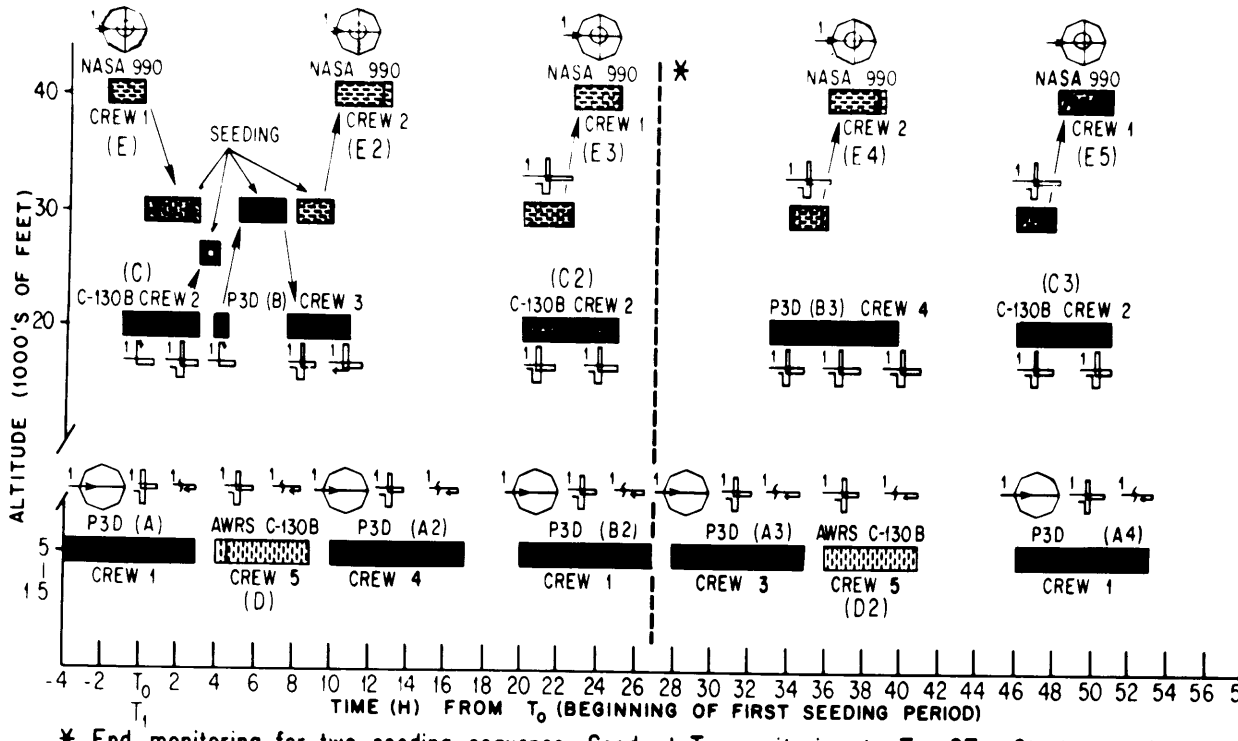

* End monitoring for two seeding sequence. Seed at T_0 monitoring to $T_0 + 27$. Start second monitoring at $T_0 + 44 = T_1 - 4$, monitor to $T_1 + 27$

Figure 30.--Stormfury aircraft employment timetable for the multiple seeding experiment.

On the basis of past experiments, particularly Hurricane Debbie, and observations of natural variabilities in storm structure and intensity, including the rapid recovery of storms after they have been modified by passage over small land masses, it is believed that no significant or detectable effects of the seeding will remain 16 to 24 h after the seeding. This means that selection criteria would preclude a populated land mass from experiencing any detectable effects of the seeding during the experimental phase of this research program.

5. POTENTIAL BENEFITS

If the Stormfury hypothesis proves correct, we can establish a practical technology for moderating severe tropical cyclones. The primary direct benefit of such a technology would be a 10% to 15% reduction in the maximum windspeeds of a severe tropical cyclone. At first glance, such a reduction would appear insufficient to bring about significant reductions in the damage caused by such a storm. However, the force of the wind varies with the square of the windspeed. (A windspeed of 50 m s^{-1} exerts four times the force of a windspeed of 25 m s^{-1}.) Therefore, a 10% to 15% reduction in the windspeed would result in a 20% to 30% reduction in the force of the wind with at least a similar reduction in damage caused by wind. In fact, several studies indicate that the reduction of damage could be significantly larger. One such study (Boyd et al., 1971) of hurricane damage in the United States indicated that the dollar damage varies as the fourth power of the wind; that

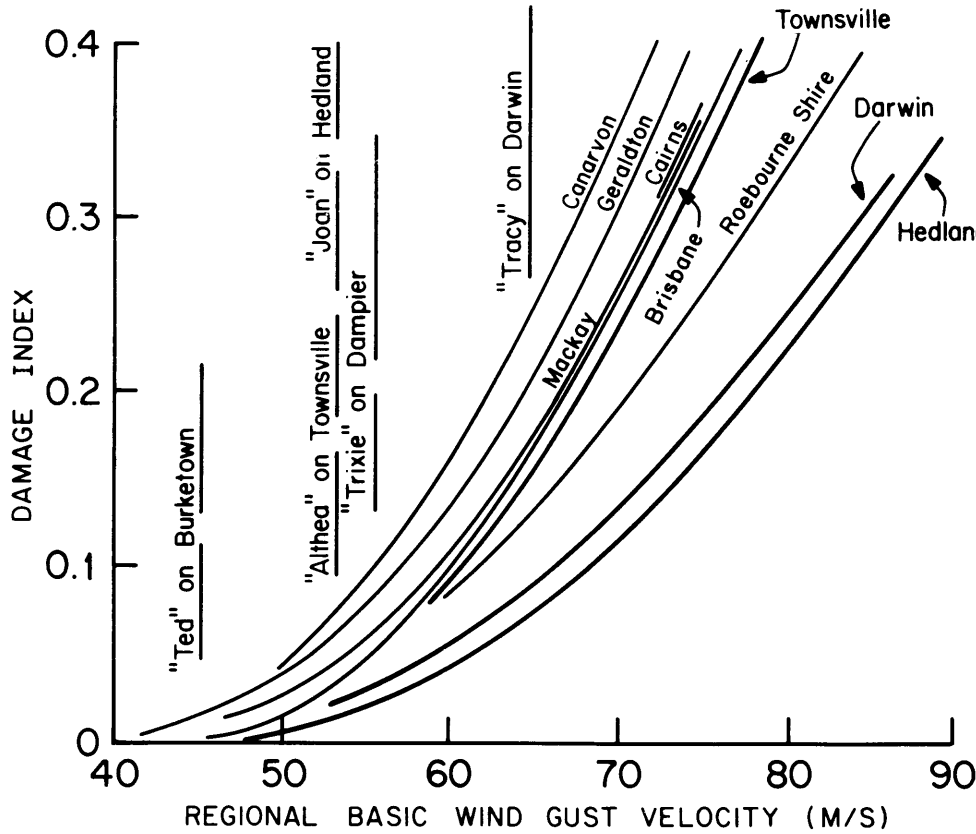

Figure 31.--Damage index for various Australian locations and building types (after Leicester and Beresford, 1978). Index is the ratio of repair cost to initial cost, assuming constant building costs.

is, a reduction of windspeed from 50 to 45 m s^{-1} would result in a 65% reduction in total damage. A similar study conducted in Australia by Dorman and Bubb (1978) concluded that "a reduction of average wind speed of 10% would cause the estimate of average annual damage to be halved." This feature is illustrated in fig. 31, which shows a damage index for buildings as a function of wind for various locations and building types in Australia. Of course, actual values in all cases would depend on threshold values of windspeed in relation to the types of structures encountered and the actual windspeeds involved.

Losses valued at more than $1 billion from single storms within the United States are not unusual. (In 1979 Hurricane Frederic caused damage of $2.3 billion.) Since coastal populations continue to increase, it is likely that the frequency of such large storm-related losses will increase. Similar conditions exist in other locations around the world. The percentage of damage caused by the three factors (wind, storm surge, inland flooding) varies considerably from storm to storm. However, a conservative estimate of the effect of a 10% to 15% reduction of the maximum windspeed for an average hurricane striking the United States coastline would be a savings of $100 to $200 million because of a decrease in wind alone, an undetermined savings because of a storm surge reduction, and no change in the damage resulting from inland flooding caused by rainfall.

The ratio of potential direct benefit to cost derived from these conservative figures, is quite large. For instance, if the Stormfury hypothesis proves correct, it is likely that the developed technology would be applied during the 24-h period preceding storm landfall. The cost for conducting operational seeding similar to that described earlier for this experiment, but excluding the extensive monitoring required for research, would be approximately $300,000 for the seeding agent and $30,000 to $40,000 for the flight hours required to conduct the seeding. A comparison of this cost with the potential savings of more than $100 to $200 million results in a benefit-to-cost ratio between 300:1 and 600:1. This figure does not include the potential saving of lives.

Another major potential benefit of this program is the comprehensive documentation of hurricane structure. The detailed study of these data sets should lead to improved understanding of tropical cyclones and, it is hoped, to improved forecasts and warnings.

6. SUMMARY

The Stormfury hypothesis may offer an opportunity to mitigate the destruction caused by tropical cyclones. Background studies, theoretical calculations, and exploratory experiments indicate that the hypothesis is scientifically plausible. Experiments to test the hypothesis appear to be logistically feasible and not likely to have significant and/or detectable negative effects. However, verification or repudiation of the hypothesis can be accomplished only by conducting actual field experiments.

7. ACKNOWLEDGMENTS

The author gratefully acknowledges the contributions of the staffs of the National Hurricane Research Laboratory, Research Facilities Center, reconnaissance crews of the Air Force and Navy, and many others whose work has been cited in this paper. Special acknowledgment is given to Richard Knight, National Climatic Center, for assistance with two of the studies contained in the appendices and to Brian Jarvinen, of the National Hurricane Center, for assistance with the SPLASH model runs.

8. REFERENCES

Boyd, D. W., R. A. Howard, J. E. Matheson, and D. W. North, 1971. Decision analysis of hurricane modification. Stanford Research Institute Report, 208 pp.

Brunt, A. T., 1966. Rainfall associated with tropical cyclones in the Northeast Australian Region. Aust. Meteorol. Mag. 14:85-109.

Dorman, C. M. L., and C. T. J. Bubb, 1978. Estimating insurance risk in tropical cyclone areas. Part 1. Commonwealth of Australia, Dept. of Housing and Construction, Canberra, 21 pp.

Frank, W. M., 1976. The structure and energetics of the tropical cyclone. Atmos. Sci. Paper 258, Dept. of Atmos. Sci., Colo. State Univ., Fort Collins, 180 pp.

Gentry, R. C., 1970. Hurricane Debbie modification experiments, August 1969. Science 168(3930):473-475.

Gentry, R. C., 1974. Hurricane modification. In Weather and Climate Modification, W. N. Hess (ed.), Wiley, New York, 497-521.

George, J. E., 1975. Tropical cyclone motion and surrounding parameter relationships. Atmos. Sci. Paper 241, Dept. of Atmos. Sci., Colo. State Univ., Fort Collins, 105 pp.

Griffith, C. G., W. L. Woodley, P. G. Grube, D. W. Martin, J. Stout, and D. N. Sikdar, 1978. Rain estimation from geosynchronous satellite imagery--visible and infrared studies. Mon. Wea. Rev. 106:1153-1171.

Hawkins, H. F., 1971. Comparison of results of the Hurricane Debbie (1969) modification experiments with those from Rosenthal's numerical model simulation experiments. Mon. Wea. Rev. 99:427-434.

Herndon, A., W. L. Woodley, A. H. Miller, A. Samet, and H. Senn, 1973. Comparison of gage and radar methods of convective precipitation measurement. Tech. Memo. ERL OD-18, NOAA Environmental Research Laboratories, Boulder, Colo., 57 pp.

Jelesnianski, C. P., and A. D. Taylor, 1973. A preliminary view of storm surges before and after storm modifications. Tech. Memo. ERL WMPO-3, NOAA Environmental Research Laboratories, Boulder, Colo., 33 pp.

Jones, R. W., 1976. A preliminary estimate of a tropical cyclone track change caused by artificial enhancement of convective heat release. Tech. Memo. ERL WMPO-27, NOAA Environmental Research Laboratories, Boulder, Colo., 23 pp.

Jones, R. W., 1977. Vortex motion in a tropical cyclone model. J. Atmos. Sci. 34:1518-1527.

Knight, R. W., and G. W. Brier, 1978. A technique for evaluating the effectiveness of hurricane modification experiments. J. Appl. Meteorol. 17:222-227.

Kuo, H. L., 1969. Motions of vortices and circulating cylinders in shear flow with friction. J. Atmos. Sci. 26:390-398.

Leicester, R. H., and F. D. Beresford, 1978. The resistance of Australian housing to wind forces. Estimating insurance risk in tropical cyclone areas, Part III, Commonwealth of Australia, Dept. of Housing and Construction, Canberra, 24 pp.

Miller, B. I., 1958. Rainfall rates in Florida hurricanes. Mon. Wea. Rev. 86:258-264.

Milton, D., 1978. The rainfall from tropical cyclones in Western Australia. Working Papers of the Dept. of Geography, Univ. of Western Australia, Perth, 61 pp.

Neumann, C. J., 1972. An alternate to the HURRAN tropical cyclone forecast system. Tech. Memo. NWS SR-62, NOAA National Weather Service, Fort Worth, Texas, 24 pp.

Neumann, C. J., J. R. Hope, and B. I. Miller, 1972. A statistical method of combining synoptic and empirical tropical cyclone prediction systems. Tech. Memo. NWS SR-63, NOAA National Weather Service, Coral Gables, Florida, 32 pp.

Rosenthal, S. L., 1971. A circularly symmetric primitive-equation model of tropical cyclones and its response to artificial enhancement of the convective heating functions. Mon. Wea. Rev. 99:414-426.

Rosenthal, S. L., and M. Moss, 1971. Numerical experiments of relevance to Project Stormfury. Tech. Memo. ERL NHRL-95, NOAA Environmental Research Laboratories, Boulder, Colo., 52 pp.

Schoner, R. W., and S. Molansky, 1956. Rainfall associated with hurricanes. NHRP Report 3, U.S. Dept. of Commerce, National Hurricane Research Laboratory, Coral Gables, Fla., 305 pp.

Senn, H. V., 1974. Quantizing 3- and 4-cm radar hurricane precipitation data. Final Rep. to NOAA, NHRL Contract No. 03-4-022-98, 10 pp.

Sheets, R. C., 1969a. Preliminary analysis of cloud physics data collected in Hurricane Gladys (1968). Project Stormfury Annual Report, 1968, U.S. Dept. of Commerce and U.S. Dept. of Navy, Appendix D, National Hurricane Research Laboratory, Coral Gables, Fla., D1-D11.

Sheets, R. C., 1969b. Computations of the seedability of clouds in a hurricane environment. Project Stormfury Annual Report, 1968, U.S. Dept. of Commerce and U.S. Dept. of Navy, Appendix E, National Hurricane Research Laboratory, Coral Gables, Fla., E1-E5.

Sheets, R. C., 1970. Applications of Bayesian statistics for Stormfury results. Project Stormfury Annual Report, 1969, U.S. Dept. of Commerce and U.S. Dept. of Navy, Appendix H, National Hurricane Research Laboratory, Coral Gables, Fla., H1-H16.

Sheets, R. C., 1973. Analysis of Hurricane Debbie modification results using the variational optimization approach. Mon. Wea. Rev. 101:663-684.

Sheets, R. C., and N. E. LaSeur, 1979. Project Stormfury/Present status - future plans. World Meteorol. Org. Bull. 1:17-23.

Simpson, J., G. W. Brier, and R. H. Simpson, 1967. Stormfury cumulus seeding experiment 1965: statistical analysis and main results. J. Atmos. Sci. 24:508-521.

Simpson, R. H., and J. S. Malkus, 1964. Experiments in hurricane modification. Sci. Amer. 211:27-37.

Simpson, R. H., M. R. Ahrens, and R. D. Decker, 1963. A cloud seeding experiment in Hurricane Esther. National Hurricane Research Project Report No. 60, Coral Gables, Fla., 30 pp.

Simpson, R. H., A. L. Sugg, and staff, 1970. The Atlantic hurricane season of 1969. Mon. Wea. Rev. 98:295-306.

Woodley, W. L., 1970. Precipitation results from a pyrotechnic cumulus seeding experiment. J. Appl. Meteorol. 9:242-257.

Appendix A: Effects of Seeding on Tropical Cyclone Motion

Richard W. Knight* and Robert C. Sheets

A.1 INTRODUCTION

The question of what effects the seeding of a storm has on the storm's motion remains unanswered quantitatively, since not enough actual seeding cases have taken place to obtain a statistically significant analysis. However, we can make some qualitative assessments based on the movements of the storms seeded since experiments began in 1961.

Numerical-model storm modification simulations (Rosenthal and Moss, 1971) and analyses of the two Hurricane Debbie experiments (Gentry, 1970; Sheets, 1973) indicate that the maximum changes in the storm structure should occur soon after the seeding. Also, the storm should start to return to its natural state within 6 to 18 h after seeding. If the storm motion is modified by seeding, it seems reasonable to expect the anomalous motion to begin soon after seeding (within 6 to 12 h). Therefore, the 12- and 24-h movement forecasts made immediately before the seeding experiment should provide good indications of whether subsequent erratic movements had taken place.

A.2 METHOD

Actual movements of the four hurricanes seeded in the Stormfury program were compared with predicted movements. The two means of comparison were official forecasts of the National Hurricane Center (NHC) and NHC's objective CLIPER (CLImatology and PERsistence) system forecasts (Neumann et al., 1972). CLIPER is a forecasting technique that uses climatology and persistence through a series of nonlinear multiple regression equations fitted to predictors derived from NHC's data base on Atlantic and Caribbean storms. This system, requiring inputs of the current storm motion, location, maximum wind, and the past 12-h storm movement, produces one of the best short-term movement forecasts currently used operationally by NHC when the exact position and motion of the storm are known. On the average, CLIPER explains more than 90% of the 12-h motion variance (Neumann et al., 1972). The accuracy of CLIPER, as well as of other objective techniques that do not include synoptic-scale structure, suffers greatly during recurvature periods. The largest errors in the official forecasts also appear during periods of rapid changes in the storm's direction of motion.

The CLIPER forecast scheme was applied at 12-h intervals to obtain 12- and 24-h forecasts for several days around each seeding period. The official 12- and 24-h forecasts were also tabulated for the same periods. Comparisons were then made with the actual movements of the hurricanes during the seeding and nonseeding periods.

*Currently affiliated with the National Climatic Center, Asheville, N.C.

A.3 RESULTS

The CLIPER objective forecasts of storm tracks were generally accurate on all four storms. The mean 12-h forecast error was <55 km for each storm track, and the mean 24-h error was ≤150 km.

Errors in forecasts relating to Hurricane Esther are listed in table A-1. For September 16, 1961, the official forecast, made just before seeding, was to the left of the actual track; the CLIPER forecast was to the right (fig. A-1). Both the official and CLIPER forecasts for September 17, 1961, made just before seeding, were slightly to the left of the actual track.

Hurricane Beulah (1963) was seeded on August 23 and 24. The forecast errors are shown in table A-2. Figure A-2 indicates that Hurricane Beulah moved on a relatively smooth north-northwest track during the period around the times of the seedings. During the early periods, large errors resulted from a forecast westward movement. The CLIPER forecasts, however, were quite good and predicted a north-northwest track.

Hurricane Debbie (1969) was seeded on two occasions. These experiments were conducted in a manner similar to that proposed for future experiments, and the evidence is quite strong that a modification of the storm may have been achieved. Table A-3 lists the forecast errors for August 16 through 23. The errors in forecasts made just before seeding on August 18 are relatively small. However, errors were relatively large for official forecasts on August 19 and 20. The main reasons for errors were slight changes in the direction of storm movement that occurred just before the seeding on August 18 and the recurvature period from August 20 to 21 (fig. A-3). Note that the official forecasts (occurring 10 and 22 h after the seeding began on August 18) had errors of only 67 km and 54 km, respectively. In this case, the official forecast, although too extreme, correctly predicted a change in the direction of the storm movement between the 12- and 24-h verification periods. The forecasts made at 0000Z on August 19 correctly predicted the direction of storm movement, but not the speed. As a result there were large errors. The next set of official forecasts issued at 1200Z on August 19 were slightly off, both in direction and speed, but the CLIPER forecast was quite accurate.

The CLIPER forecast based on the 0000Z data on August 20, 1969, was extremely accurate. However, the remainder of the forecasts through the period of recurvature exhibited relatively large errors, because neither the CLIPER nor official forecasts correctly predicted the recurvature in the relatively data-void region of the North Atlantic.

Hurricane Ginger (1971) was seeded on September 26 and 28. (The storm was unsuitable for the primary Stormfury experiment. Therefore, the rain-sector experiment was conducted on an area well away from the storm center.) The storm had undergone considerable erratic movement before the Stormfury experiments. At the time of the first experiment, the storm was drifting slowly westward (fig. A-4). The official forecast predicted a southward drift, which resulted in large errors for the forecast with an initial time of 1200Z on September 26. The CLIPER forecast picked up the westward movement, with the result that the 12- and 24-h errors were only 15 km and 89 km, respectively, for this same period (table A-4). The errors for the official forecast with an initial time of 1200Z on September 28 were below average, and the CLIPER forecasts for the same period were slightly above average.

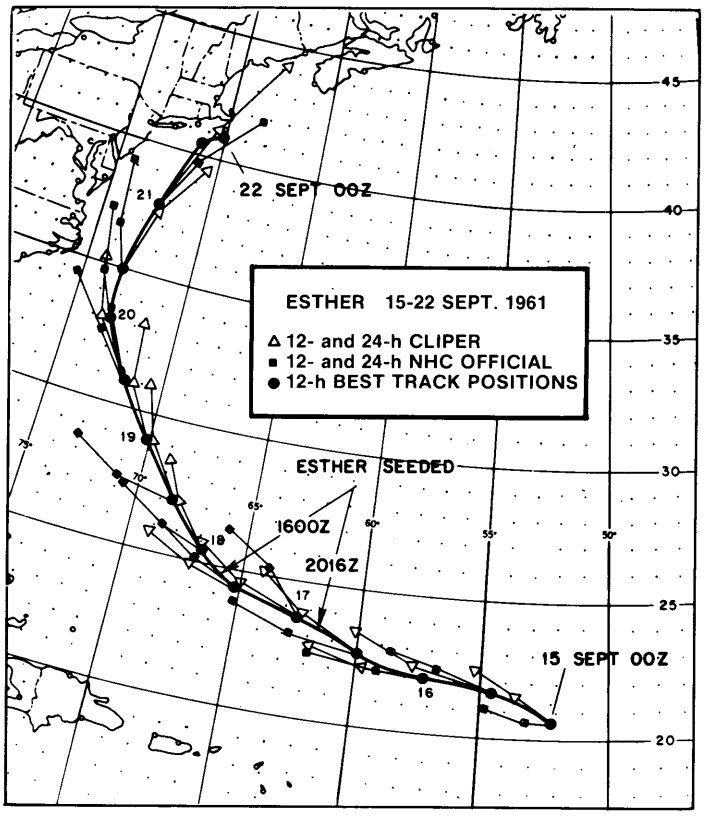

Figure A-1.--Storm track and forecast vector movement for Hurricane Esther (1961).

Table A-1.--Errors in storm track forecasts for Hurricane Esther, September 1961

Date/Time	Errors (km)			
	Official forecast†		CLIPER forecast	
	12-h	24-h	12-h	24-h
15/12Z	80	124	54	89
16/00Z	76	146	48	117
16/12Z*	83	59	24	128
17/00Z	158	152	46	55
17/12Z*	30	100	59	128
18/00Z	100	208	59	108
18/12Z	208	300	9	124
19/00Z	24	48	48	132
19/12Z	50	178	55	96
20/00Z	67	196	11	91
20/12Z	172	295	57	102
21/00Z	69	182	89	410
21/12Z	245	515	117	336
22/00Z	163	371	69	180
Average	108	204	52	148

*Forecasts with initial times just before seeding.
†Official 24-h forecast errors for all storms (1961): mean = 295 km; standard deviation = 213 km.

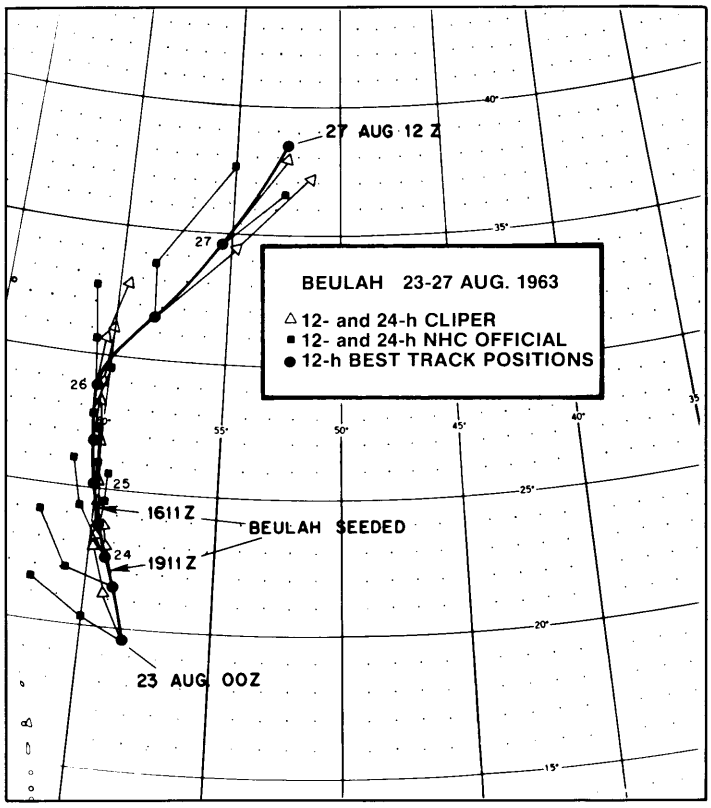

Figure A-2.--Storm track and forecast vector movement for Hurricane Beulah (1963).

Table A-2.--Errors in storm track forecasts for Hurricane Beulah, August 1963

Date/Time	Errors (km)			
	Official forecast†		CLIPER forecast	
	12-h	24-h	12-h	24-h
23/00z	167	298	30	61
23/12Z*	174	237	44	89
24/00Z	106	135	35	59
24/12Z*	91	165	15	15
25/00Z	95	171	33	80
25/12Z	122	269	15	161
26/00Z	254	551	196	421
26/12Z	297	228	74	195
Average	163	256	54	133

*Forecasts with initial times just before seeding.
†Official 24-h forecast errors for all storms (1963): mean = 260 km; standard deviation = 165 km.

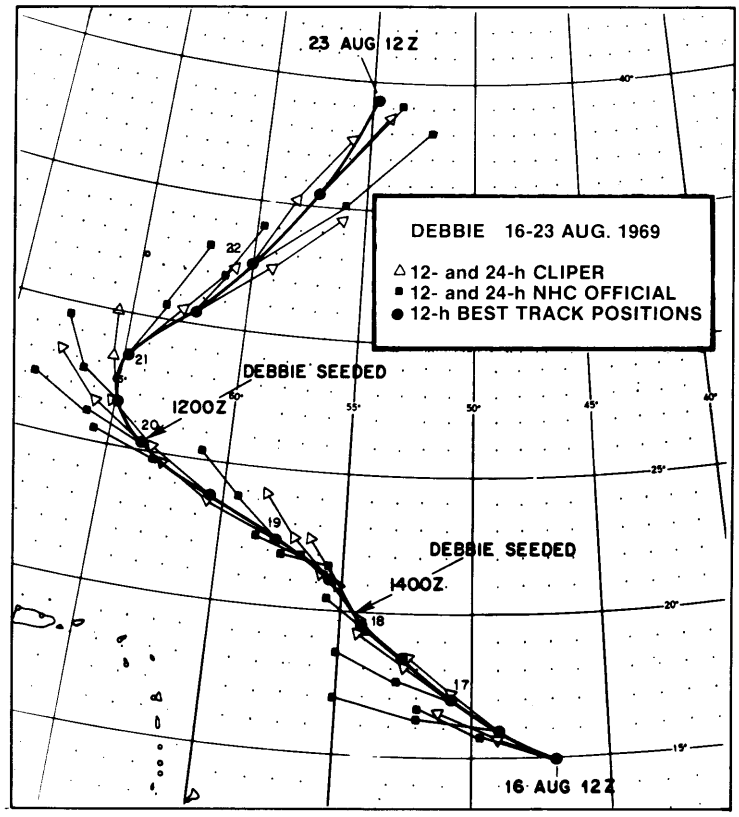

Figure A-3.--Storm track and forecast vector movement for Hurricane Debbie (1969).

Table A-3.--Errors in storm track forecasts for Hurricane Debbie, August 1969

Date/Time	Errors (km)			
	Official forecast†		CLIPER forecast	
	12-h	24-h	12-h	24-h
16/12Z	89	132	20	61
17/00Z	145	297	15	15
17/12Z	82	146	35	35
18/00Z	24	78	30	46
18/12Z*	67	54	24	167
19/00Z	111	250	85	237
19/12Z	111	252	24	87
20/00Z	67	135	43	39
20/12Z*	122	386	100	276
21/00Z	180	526	59	328
21/12Z	135	193	69	87
22/00Z	115	260	96	148
22/12Z	117	276	96	202
23/00Z	115	287	96	282
23/12Z	202	465	33	218
Average	111	248	54	148

*Forecasts with initial times just before seeding.
†Official 24-h forecast errors for all storms (1969): mean = 260 km; standard deviation = 154 km.

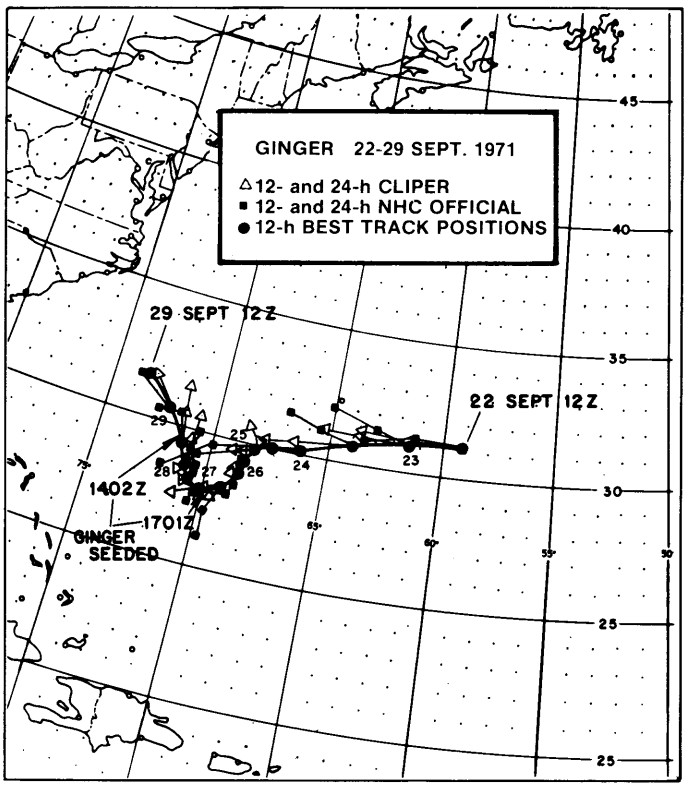

Figure A-4.--Storm track and forecast vector movement for Hurricane Ginger (1971).

Table A-4.--Errors in storm track forecasts for Hurricane Ginger, September 1971

Date/Time	Errors (km)			
	Official forecast†		CLIPER forecast	
	12-h	24-h	12-h	24-h
22/12Z	19	52	11	87
23/00Z	117	241	44	156
23/12Z	141	174	24	70
24/00Z	124	254	39	78
24/12Z	174	354	46	135
25/00Z	11	83	24	113
25/12Z	95	174	15	72
26/00Z	59	119	9	59
26/12Z*	96	246	15	89
27/00Z	59	143	20	30
27/12Z	59	135	30	44
28/00Z	133	163	163	126
28/12Z	50	163	48	170
29/00Z	104	211	19	132
Average	83	178	35	96

*Forecasts with initial times just before seeding.
†Official 24-h forecast errors for all storms (1971): mean = 208 km; standard deviation = 124 km.

A.4 SUMMARY AND CONCLUSIONS

No obvious anomalous movements were detected that could be associated with any of the eight seeding events. Also, no obvious quantitative differences were noted for seeded periods versus nonseeded periods where the standards used were the official forecasts and the results of an objective forecast scheme (CLIPER). That is, any effect on the movement of the storm, possibly caused by seeding, is well within the natural-variability range. The number of cases available for study makes it impossible to ascertain with any reasonable degree of certainty whether the motion of the storm is affected in some small way by seeding. However, if the cases studied here are at all representative of seeded storms, seeding will not produce large changes in the movement of the storm.

Appendix B: Tropical Cyclone Rain Estimation From Geosynchronous Satellite Imagery

Griffith et al. (1978) developed a technique for estimating rainfall from geosynchronous-satellite imagery. The technique was applied to several hurricanes to evaluate hurricane rainfall characteristics versus intensity. Extracts, interpretations, and conclusions from their study are presented here.

Table B-1 lists estimates of hurricane rain volume and average rain depth (storm area determined by threshold 80-digital-count contour) for six storms. The rain volume for Hurricane Debbie increased slightly on August 19 and decreased on August 20 and 21. The other storms showed similar variations with time as well as changes in the central pressure. There appears to be no relationship between changes of rainfall and changes of pressure; that is, some increases in rainfall were associated with decreases in pressure, and some decreases in rainfall were associated with increases in pressure (see figs. B-1 and B-2).

In a detailed study of Hurricane Debbie, radial profiles of cloud brightness were computed along with associated daily mean rain depths before, during, and after the two seeding events (August 18 and 20). The results (not shown) indicate that the profiles and their changes with time are little different for August 18 and 20 (days of seedings) and for August 19 and 21 (nonseeding days) (Griffith et al., 1978, personal communication).

Table B-1.--Daily hurricane rain estimates from satellite imagery*

Day relative to minimum sea level pressure	Storm parameter	Hurricane					
		Debbie (1969)	Celia (1970)	Edith (1971)	Agnes (1972)	Carmen (1974)	Fifi (1974)
-3	$\bar{P}$ (mb)				1000		1000
	Rain volume ($m^3 x 10^{11}$)				1.03		1.00
	Average depth (mm)				143		134
-2	$\bar{P}$ (mb)	974	975	1001	995	998	984
	Rain volume ($m^3 x 10^{11}$)	0.29	0.75	0.32	0.91	0.40	1.17
	Average depth (mm)	59	65	122	131	112	145
-1	$\bar{P}$ (mb)	964	980	989	985	983	974
	Rain volume ($m^3 x 10^{11}$)	0.30	0.14	0.39	1.00	0.59	1.43
	Average depth (mm)	80	33	99	135	164	108
0	$\bar{P}$ (mb)	956	969	962	982	949	974
	Rain volume ($m^3 x 10^{11}$)	0.19	0.07	0.14	0.95	0.53	1.41
	Average depth (mm)	76	31	35	101	113	101
+1	$\bar{P}$ (mb)	961	1000	-		965	996
	Rain volume ($m^3 x 10^{11}$)	0.17	0.04	0.09		0.28	0.90
	Average depth (mm)	66	28	25		75	57

*Griffith et al. (1978)

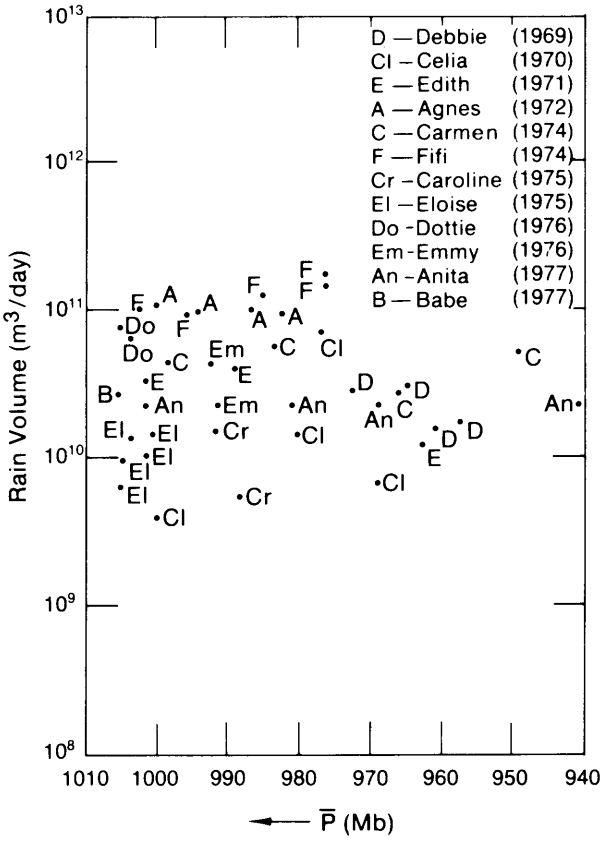

Figure B-1.--Daily hurricane rain volume (m^3/day) as a function of mean daily sea level pressure (mb) for selected storms (after Griffith et al., 1978). Daily rain volumes were calculated from ATS-3 images.

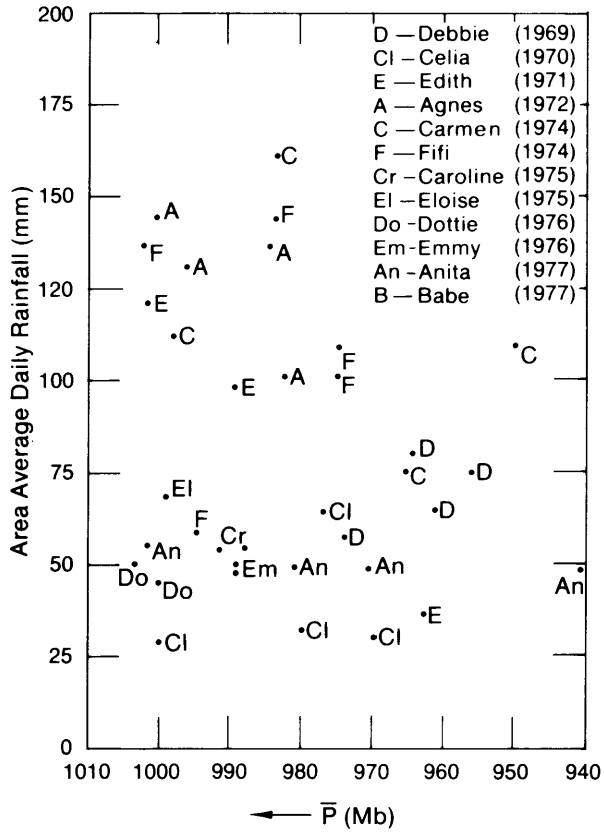

Figure B-2.--Area-averaged daily hurricane rainfall (mm) as a function of mean daily sea level pressure (mb) for selected storms (after Griffith et al., 1978). Rain depths were calculated from satellite-derived rain volumes and satellite-derived storm area, measured at the 80-digital-count contour.

Appendix C: Simulations of Tropical Cyclone Rainfall Distribution Changes Based on the Stormfury Hypothesis

Robert C. Sheets and Richard W. Knight*

C.1 INTRODUCTION

A major question about the effects of hurricane modification experiments concerns the changes that will take place in the precipitation associated with the storm. The Stormfury hypothesis calls for a redistribution of convection only near the storm center as a result of the change in location of the major vertical mass transport. This process was illustrated in figs. 2 and 3, where the original eyewall is shown as it dissipates and a new, larger, but weaker (on the assumption of no large increase in mass inflow), eyewall forms at a slightly greater distance from the storm center. The result, of course, is that precipitation is reduced or eliminated in the region of the original eyewall and slightly increased in the seeded area because of the assumed cloud growth. The Stormfury assumption about redistributing convection is based on cloud-seeding experiments carried out over South Florida on individual clouds (Woodley, 1970), which demonstrated that rainfall rates can be increased using the dynamic seeding of the Stormfury experiments. The Stormfury hypothesis further states that a seeded storm should return to its natural state within 6 to 18 h after the seeding ends. (This is based primarily on results from Hurricane Debbie.) With these considerations in mind, the study described here was conducted in an attempt to simulate changes in the net rainfall distribution that might be expected to result from the tropical cyclone modification experiments. Some of the hypothetical changes were chosen to coincide with the current Stormfury hypothesis; others were chosen to represent extremes.

C.2 METHOD

A hypothetical radar PPI precipitation pattern composited by Senn (1974) was used as the model storm (fig. C-1). This composite is based on radar data obtained from four hurricanes and can be considered representative of a typical over-water hurricane as observed from several 10-cm radars. Four levels of PPI contouring are depicted. Each contour level was assigned the equivalent precipitation rate for the NHC WSR-57M radar (Herndon et al., 1973, table C-1).

Precipitation rates in the model storm were interpolated onto a square grid having an area of 408 km^2 and grid points 8 km apart. An east-west line (A-A) defined by 51 grid points 8 km apart was located north of the 408 km^2 grid (top of fig. C-1). The storm, assumed to be in steady state, was moved northward at 18.5 km h^{-1} across this line. The rainfall was then summed at each of the 51 grid points on the line for the period of the storm's passage.

*Currently affiliated with the National Climatic Center, Asheville, N.C.

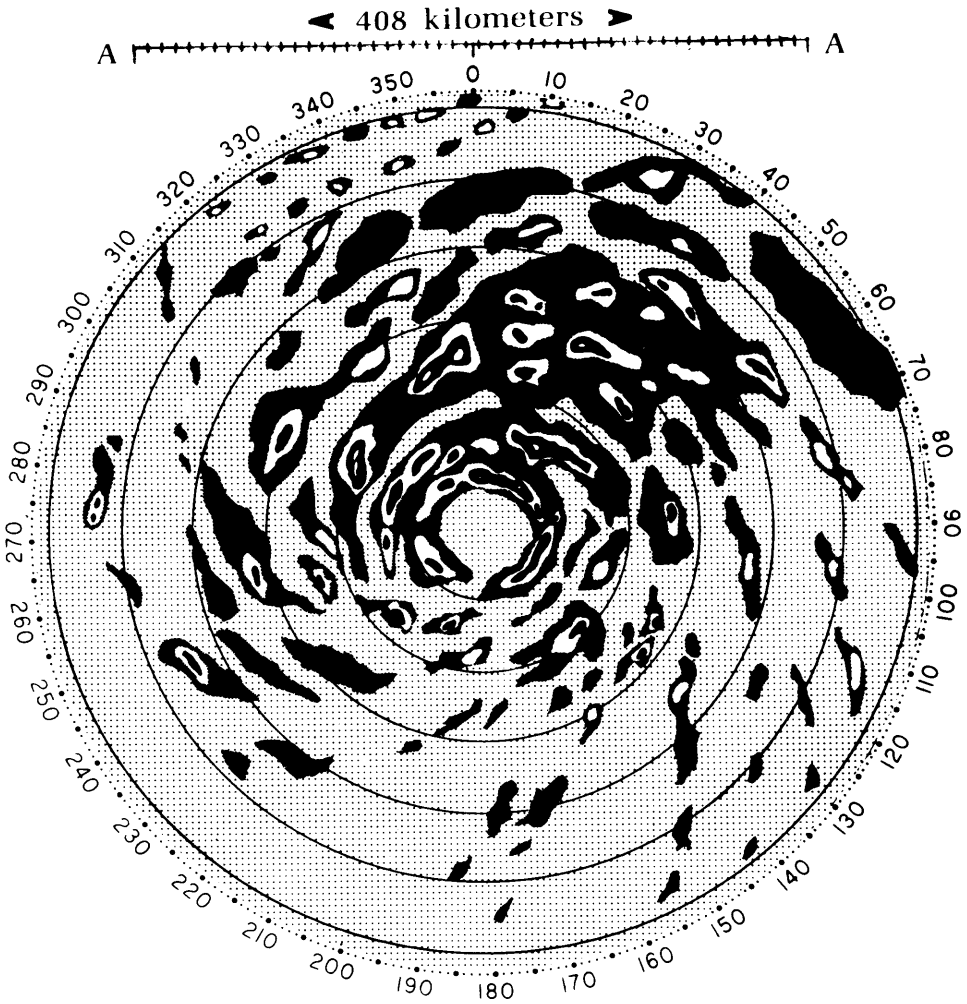

Figure C-1.--A hypothetical improved radar PPI precipitation pattern (after Senn, 1974). Range markers are at 40-km intervals.

The resulting precipitation (unmodified storm) is listed as the initial precipitation (P_I) in the figures presented later. The precipitation rates in successive storms were modified by changing the precipitation rates in various portions of the original storm to correspond to hypothetical seeding experiments. Each modified storm was moved across the collection line as before, and the new precipitation distribution (P_M) was compared with that of the original storm. The storm was assumed to stay in steady state, that is, in its maximum modified state, for the entire 20 h required for the storm to pass over the area where the rainfall was "collected." If the actual modified period is as expected (6 to 18 h) then an assumed maximum modified state for a 20-h period should result in an overestimate of changes.

The tests of significance used to compare the results were the Kolmogorov-Smirnoff and the Wilcoxon rank sum test (both two-sided). Nonparametric tests were used because the original precipitation distribution was not normal and could not easily be transformed into a normal distribution. The tests were used to decide whether to accept the null hypothesis (H_0: $P_I = P_M$), which states that the precipitation sample from the initial storm and the modified storm came from the same population.

Table C-1.--Radar equivalent precipitation rates for NHC WSR-57M*†

Contour level	$10 \log_{10} Z$ (dBZ)	Rainfall rate ($mm\ h^{-1}/in\ h^{-1}$)
1	18.3	.254/0.01
2	29.5	2.286/0.09
3	40.7	13.716/0.54
4	45.5	30.226/1.19
5	50.3	66.549/2.62
6	56.7	190.754/7.51

*Obtained from relation $Z = 300\ R^{1.4}$.
†Herndon et al., 1973.

C.3 RESULTS

The statistical tests used were not able to reject the null hypothesis; that is, the initial and modified precipitation were from the same population, at the 5% level, unless the precipitation rates over large areas of the storm were changed by factors of 3 or 4. For more realistic values of seeding-induced rainfall changes, no statistically significant difference could be detected between the initial and modified precipitation distribution when summed over the entire storm. Although the statistical tests indicate that the initial and modified precipitation patterns were from the same populations for all reasonable changes in rainfall, the Stormfury experiments are also intended to have very little effect on the accumulated rainfall at individual locations. It is important, therefore, to determine the changes that would be experienced at a given point because of these hypothetical changes in the rainfall rates for given area segments of modified storms.

Figures C-2 (a-d) show the accumulated rainfall distribution along the line illustrated in the upper portion of fig. C-1. The initial (unmodified) cumulative distribution (P_I) is illustrated by the light shaded area and the deviations from P_I resulting from the simulated modification are indicated by the dark shaded areas. The modifications to the initial precipitation pattern are indicated in the table at the top of each figure. The percentage rainfall rate changes were applied in annular rings between the radial distances indicated, which were completely encircling the storm center.

Figure C-2 (a) illustrates the case that might be reasonably expected under the current Stormfury hypothesis, that is, a significant reduction in the initial eyewall location and an increase in the potential seeding area. The result is that only minor variations are observed, even with the assumption that the maximum effect lasts more than 20 h.

Figure C-2 (b) illustrates a situation similar to that depicted in fig. C-2 (a). The only change is that a considerably larger area is assumed to be convectively enhanced. However, the results again show no major alterations in the accumulated rainfall.

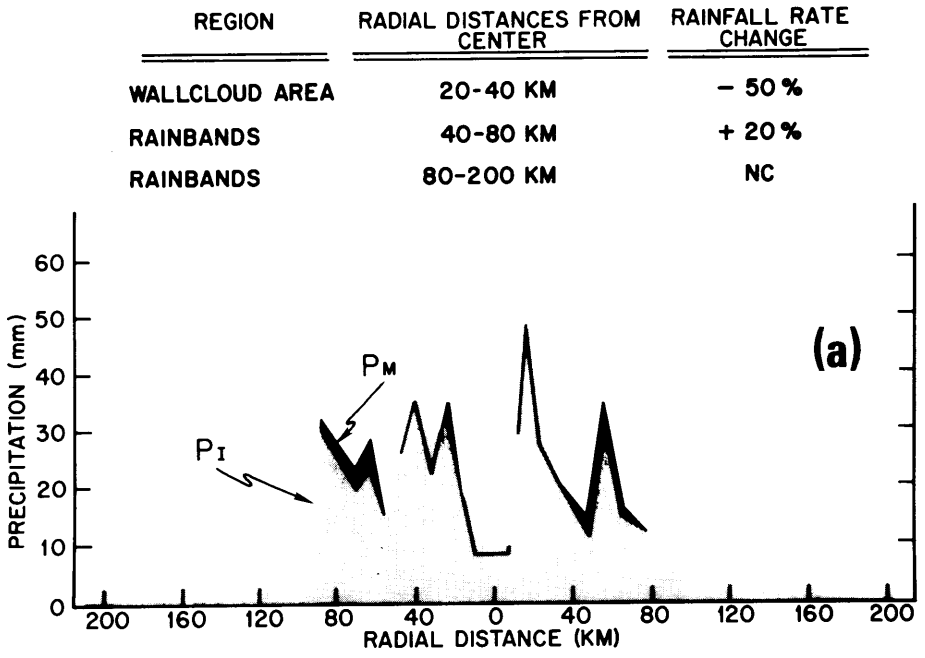

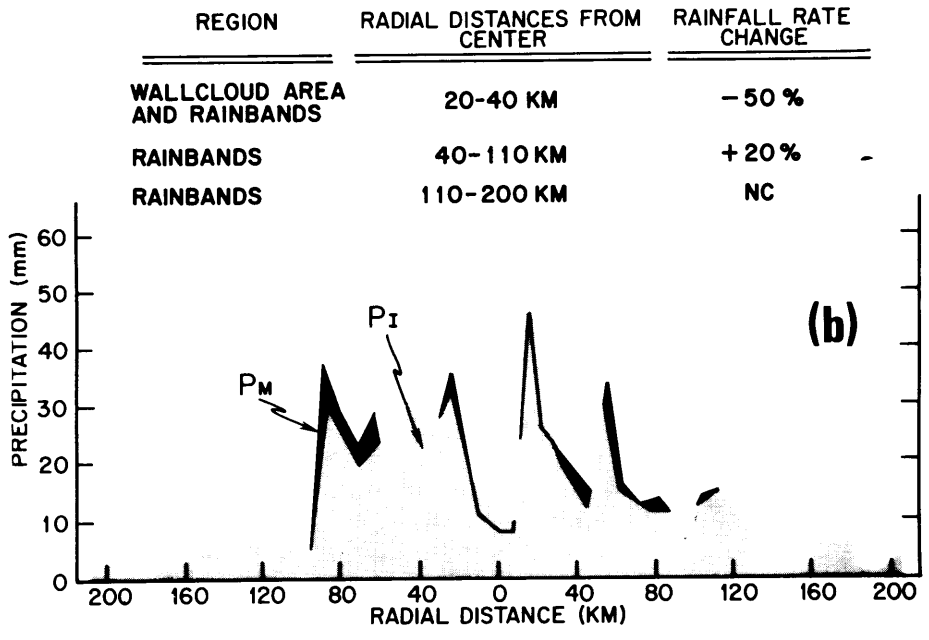

Figure C-2 (a-d).--Cumulative precipitation values as the precipitation pattern illustrated in fig. C-1 was moved over line A (fig. C-1). The initial (unmodified) distribution P_I is illustrated by the light-shaded area, and deviations from P_I resulting from the simulated modification are indicated by the dark-shaded areas P_M. Modifications are indicated in the table at the top of each example.

REGION	RADIAL DISTANCES FROM CENTER	RAINFALL RATE CHANGE
WALLCLOUD AREA AND RAINBANDS	0-48 KM	−100 %
RAINBANDS	48-72 KM	+ 21 %
RAINBANDS	72-150 KM	+ 10 %
RAINBANDS	150-200 KM	NC

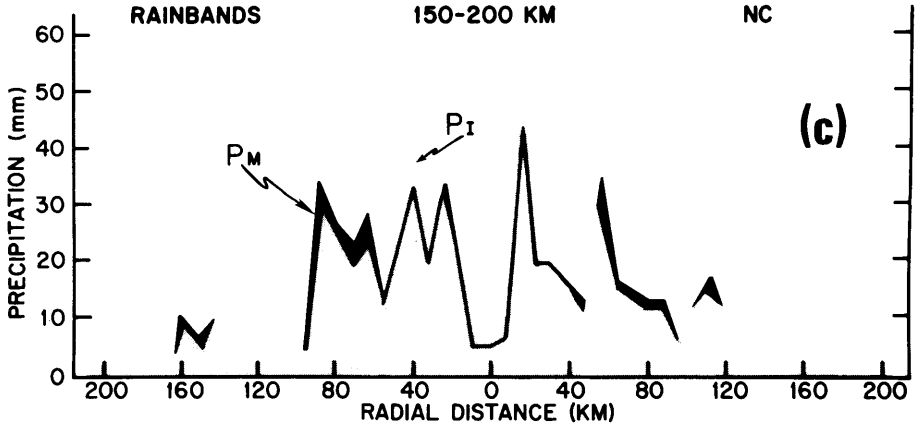

REGION	RADIAL DISTANCES FROM CENTER	RAINFALL RATE CHANGE
WALLCLOUD AREA AND RAINBANDS	20-60 KM	+40 %
RAINBANDS	60-200 KM	NC

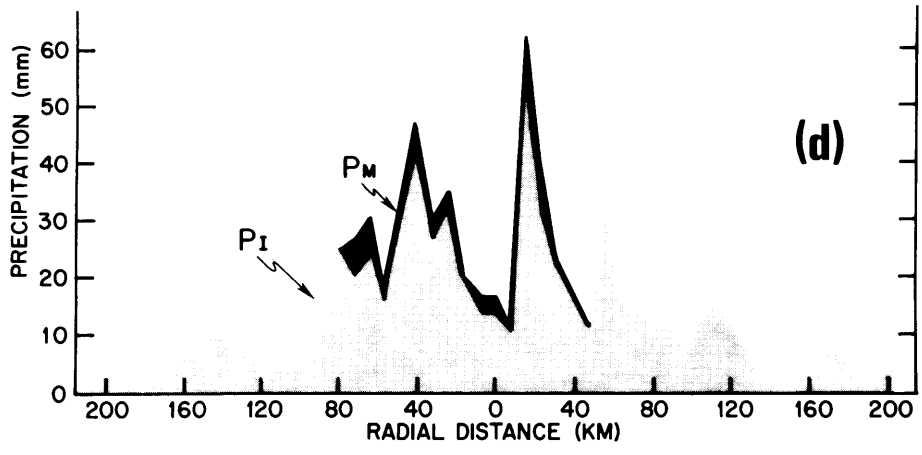

Figure C-2.--Continued.

Figure C-2 (c) starts tending toward extreme assumptions. That is, the initial eyewall is completely dissipated, and the convection is enhanced as far out as 150 km. Even with these extreme assumptions, no large changes are depicted in the accumulated rainfall.

Figure C-2 (d) resulted from extreme assumptions concerning the eyewall and inner rainbands. That is, large increases in rainfall rates are assumed over the entire inner portions of the storm with no corresponding decreases. Even with these assumptions, pointwise accumulation changes rarely exceeded 10% of the control values.

C.4 SUMMARY AND CONCLUSIONS

No major changes are observed in the cumulated point value or area-averaged rainfall when reasonable assumptions are made about alterations in the rainfall as a result of the simulated modification. Even extreme assumptions produce very few significant alterations in the accumulated rainfall. Figure C-1 reveals why. The eyewall contains only a small part of the total precipitating area of a storm and affects a given area for only a short time. It is emphasized that the assumed changes of rainfall rates were allowed to persist at their maximum rate for more than 20 h, resulting in an amplification of any cumulative changes. Verification of these results is difficult because no quantitative precipitation data have been collected in seeded storms to date. However, quantitative measurements are now possible because of the acquisition of new digitized airborne radar systems, and it is planned that this system will be used in all future experiments.

☆ U.S. GOVERNMENT PRINTING OFFICE: 1981—576-001/1203 Region no. 8

Environmental Research LABORATORIES

The mission of the Environmental Research Laboratories (ERL) is to conduct an integrated program of fundamental research, related technology development, and services to improve understanding and prediction of the geophysical environment comprising the oceans and inland waters, the lower and upper atmosphere, the space environment, and the Earth. The following participate in the ERL missions:

AL *Aeronomy Laboratory.* Studies the physics, dynamics, and chemistry of the stratosphere and the surrounding upper and lower atmosphere.

AOML *Atlantic Oceanographic and Meteorological Laboratories.* Study the physical, chemical, biological, and geological characteristics and processes of the ocean waters, the sea floor, and the atmosphere above the ocean, including tropical meteorology such as hurricanes and tropical weather systems.

ARL *Air Resources Laboratories.* Study the diffusion, transport, dissipation, and chemistry of atmospheric pollutants; develop methods of predicting and controlling atmospheric pollution; monitor the global physical environment to detect climatic change.

GFDL *Geophysical Fluid Dynamics Laboratory.* Studies the dynamics of geophysical fluid systems (the atmosphere, the hydrosphere, and the cryosphere) through theoretical analysis and numerical simulation using powerful, high-speed digital computers.

GLERL *Great Lakes Environmental Research Laboratory.* Studies hydrology, waves, currents, lake levels, biological and chemical processes, and lake-air interaction in the Great Lakes and their watersheds; forecasts lake ice conditions.

NSSL *National Severe Storms Laboratory.* Studies severe-storm circulation and dynamics, and develops techniques to detect and predict tornadoes, thunderstorms, and squall lines.

OWRM *Office of Weather Research and Modification.* Conducts a program of basic and applied research to advance the understanding and define the structure of mesoscale phenomena, to improve short-range weather predictions and warnings, and to identify and test hypotheses for beneficially modifying weather processes.

PMEL *Pacific Marine Environmental Laboratory.* Monitors and predicts the physical and biochemical effects of natural events and human activities on the deep-ocean and coastal marine environments of the Pacific region.

PROFS *Prototype Regional Observing and Forecasting Service.* Evaluates and integrates advanced meteorological measurement, forecasting, and communication/dissemination technologies into functional mesoscale weather forecast system designs for transfer to operational agencies such as NWS, NESS, and FAA.

RFC *Research Facilities Center.* Operates instrumented aircraft for environmental research programs; provides scientific measurement tools, logged data, and associated information for meteorological and oceanographic research programs.

SEL *Space Environment Laboratory.* Studies solar-terrestrial physics (interplanetary, magnetospheric, and ionospheric); develops techniques for forecasting solar disturbances; provides real-time monitoring and forecasting of the space environment.

W/M *Weather Modification Program Office.* Plans and coordinates ERL weather modification projects for precipitation enhancement and severe storms mitigation.

WPL *Wave Propagation Laboratory.* Develops, and applies to research and services, new methods for remote sensing of the geophysical environment.

U.S. DEPARTMENT OF COMMERCE
National Oceanic and Atmospheric Administration
BOULDER, COLORADO 80303